NASA Contractor Report 3024

Analysis of Turbulent Free Jet Hydrogen-Air Diffusion Flames With Finite Chemical Reaction Rates

J. P. Sislian

CONTRACT NAS1-14843
AUGUST 1978

NASA

NASA Contractor Report 3024

Analysis of Turbulent Free Jet Hydrogen-Air Diffusion Flames With Finite Chemical Reaction Rates

J. P. Sislian
University of Toronto
Ontario, Canada

Prepared for
Langley Research Center
under Contract NAS1-14843

NASA
National Aeronautics
and Space Administration

Scientific and Technical
Information Office

1978

Summary

The nonequilibrium flow field resulting from the turbulent mixing and combustion of a supersonic axisymmetric hydrogen jet in a supersonic parallel ambient coflowing air stream is numerically analyzed. The effective turbulent transport properties are determined by means of the (k-ϵ) model of turbulence (two-equation model). The finite-rate chemistry model considers eight elementary reactions between six chemical species, H, O, H_2O, OH, O_2 and H_2. The governing set of nonlinear partial differential equations is solved by an implicit finite-difference procedure.

Radial distribution at two downstream locations of some important variables affecting the flow development, such as the turbulent kinetic energy, turbulent dissipation rate, turbulent scale length and viscosity, are obtained. The results show that these variables attain their peak values at the axis of symmetry. The computed distributions of velocity, temperature and mass fractions of the chemical species present give a complete description of the flow field considered.

A possible direct analytical approach to account for species-concentration fluctuations on the mean production rate of these species (the phenomenon of unmixedness) is also presented. However, the use of the method does not seem justified in view of the excessive computer time required to solve the resulting systems of equations. Comparison of species mass fractions at a distance downstream equal to eight hydrogen jet diameters without unmixedness and with it, assuming that local-equilibrium turbulence prevails in the flow field, revealed no appreciable differences in the predicted values of species mass fractions at these distances.

CONTENTS

Notation

$b_1, \ldots, b_8$	backward reaction rate constants [$m^3/kmol \cdot s$, $m^6/kmol^2 \cdot s$]
c_p	specific heat at constant pressure [$J/kg \cdot K$]
$\dot{c}_{ij}$	production rate of species i in reaction j [$kmol/m^3 \cdot s$]
$c_1, \ldots, c_7$	concentration of species [$kmol/m^3$]
$\dot{c}_K$	production rate of species K due to all chemical reactions
C	concentration of catalyst $C = \sum_{i=1}^{7} c_i$ [$kmol/m^3$]
$C_\mu, C_1, C_2, C_{g_1}, C_{g_2}$	constant coefficients appearing in turbulence model
$f_1, \ldots, f_8$	forward reaction rate constants [$m^3/kmol \cdot s$]
h_i	partial static enthalpy of species i [J/kg]
H	total (stagnation) enthalpy [m^2/s^2]
k	specific turbulent kinetic energy
ℓ	dissipation length scale
Le	Lewis number
M	molecular weight [$kg/kmol$]
p	static pressure
Pr	Prandtl number
r	radius measured from axis of jet
R	universal gas constant [$J\ kmol^{-1} \cdot K^{-1}$]
S_i	production rate of species i due to all chemical reactions divided by the total density, $S_i = \dot{c}_i/\rho$, Eq. (12)
Sc	Schmidt number
t	time
T	temperature (°K)

u	x-component of velocity
v	r-component of velocity
x	distance along central axis
x_i	unknown variables in the model equation (14)
X	catalyst
Y_i	mass fraction of species i divided by its molecular weight, $Y_i = \alpha_i/M_i$ [kmol of i/kg_{mixt}]
Y_f	mass fraction of elemental hydrogen divided by the molecular weight of atomic hydrogen
Y_x	mass fraction of elemental oxygen divided by the molecular weight of atomic oxygen
$Z_{\alpha\beta}$	second-order correlations of species concentration fluctuations
α_i	mass fractions of species i
ϵ	turbulent dissipation rate
μ	coefficient of viscosity
ρ	density
σ_k, σ_ϵ	constant coefficients appearing in the turbulence model

Subscripts

C	chemistry
D	diffusion
E	external edge of flow
i	value of quantity at initial station; number of species i = 1, ..., 7
I	internal edge of flow
K	number of species, K = 1, ..., 7
t	refers to turbulent quantity

Superscripts

*	nondimensional quantity
–	time-averaged value

1. INTRODUCTION

Chemical reactions occurring in turbulent flows are of great importance in several engineering problems, e.g., in industrial furnaces, air-breathing propulsion systems, rocket exhaust plumes, chemical lasers and dispersion of pollutants introduced into the atmosphere. The investigation of such flows is complicated by the simultaneous occurrence of fluid-mechanical and chemical effects, the reactants first mixing and then combining so as to release chemical energy. A complete analysis of such processes is a formidable task. Consequently, many simplifications are required for a solution and insight into the problem. As in all viscous flows involving chemical reactions, it is appropriate to consider two characteristic times, one associated with the turbulent diffusion process t_d and one with the chemical reaction t_r. If $t_d \gg t_r$, the reaction process is much faster than the turbulent diffusion process. Then the flow may be assumed to be in chemical equilibrium everywhere. However, in most practical situations t_d and t_r can be of the same order of magnitude and, therefore, the interplay of chemical and fluid dynamic effects must be considered. In such instances, calculations of the flow are made under the assumption that the mean rate of production of each species equals the instantaneous rate with the mean quantities such as temperature, density, and species concentration replacing their instantaneous values. This assumption does not account for the effects of turbulence on the reaction rate which may be significant in certain regions of the flow field.

In recent years the problem of free-jet turbulent mixing coupled with chemical reactions has attracted the attention of several groups of investigators (Refs. 1-12). The problem considered in all of these investigations is basically the same, viz. the turbulent mixing and combustion of a plane or axisymmetric straight primary fuel jet (or rocket exhaust plume) in a parallel ambient coflowing medium. Different investigators have approached the problem by introducing different simplifying assumptions about the turbulence model describing the turbulent-mixing process, and the chemical model describing the particular combustion process considered. Some of the authors have assumed that the flow field is in local chemical equilibrium, while others have considered the nonequilibrium effects which are determined by the chemical kinetics of the reactions involved. However, in almost all the investigations the turbulent mixing process was treated by simple "algebraic" turbulent-viscosity models or by "differential" turbulent-viscosity models. The latter involved one differential equation for the turbulent kinetic energy. The other property of turbulent motion required to determine the turbulent viscosity, viz. the length scale of turbulence, was obtained from various assumed algebraic relations.

In the present investigation the problem of turbulent mixing and combustion of a round, straight hydrogen jet in a parallel ambient coflowing air is treated by modelling: (a) the turbulent mixing process with a system of two partial differential transport equations for the turbulent kinetic energy and its dissipation rate which define the eddy viscosity, and (b) the hydrogen-air combustion process with a set of differential equations describing the finite-rate production of the species considered. For the set of reactions considered, an analytical-numerical approach, based on the use of second-order correlations of the species concentrations and their balance equations properly closed in accordance with the turbulence model used, is suggested to account

for the effects of turbulent fluctuations of species concentrations on the mean species production rate. An improved version of the CHARNAL code (Calculator of Hydrogen-Air Reactions for NASA Langley) (Ref. 13) developed at NASA Langley Research Center, was used extensively in the solution of the problem.

Radial distributions are obtained at two downstream locations of some important variables affecting the flow development such as the turbulent kinetic energy, turbulent dissipation rate, turbulent length scale and turbulent viscosity. The computed distributions of velocity, temperature and mass fractions of chemical species give a complete description of the flow field considered. The numerical predictions are compared with two sets of experimental data. Good qualitative agreement is obtained.

The continued interest shown by Professor I. I. Glass and his constructive comments throughout the course of this work is greatly appreciated. Thanks are due Dr. H. L. Beach, Jr., NASA Langley Research Center, for providing the opportunity to carry out the present research. The valuable and considerable help and cooperation obtained from Dr. J. S. Evans, NASA Langley Research Center, in performing the numerical computations throughout the course of this investigation is gratefully acknowledged. It is a pleasure to thank the Director, Professor J. H. de Leeuw, and the Staff of the Institute for Aerospace Studies, University of Toronto, for providing me with this opportunity to work at UTIAS. The assistance of Mrs. Winifred Dillon in preparing the manuscript is sincerely appreciated.

2. COMBUSTION OF HYDROGEN IN AIR AT CONSTANT PRESSURE

The importance of finite-rate chemistry in accurately predicting the flow field properties has been shown in various studies (see, for example, Refs. 1, 6, 7, 8). The accuracy of the predictions depends largely on the employed reaction mechanism. It should be noted, however, that each additional species adds to the computational difficulties associated with solving the differential equations in the mathematical model of the reacting system. The reaction mechanism for hydrogen-air combustion is fairly well established (Refs. 14-18). The rate constants for all reactions in the chain have been determined but the accuracy of these determinations can be questioned to possibly within an order of magnitude. Any inaccuracies in the rate constants are naturally carried on to the temperature and composition histories which result from a detailed analysis of the system. It has been found that eight forward and eight backward reactions involving six reacting species plus nitrogen as an inert gas* describe the essential mechanism at temperatures of interest. These are listed as follows:

1. $H + O_2 \underset{b_1}{\overset{f_1}{=\!=}} OH + O$

2. $O + H_2 \underset{b_2}{\overset{f_2}{=\!=}} OH + H$

3. $H_2 + OH \underset{b_3}{\overset{f_3}{=\!=}} H + H_2O$

4. $2\,OH \underset{b_4}{\overset{f_4}{=\!=}} O + H_2O$

* For temperatures below about 2200°K the nitrogen reactions and subsequent formation of NO and N have been shown to be unimportant (Ref. 17).

$$5.\quad H_2 + X \underset{b_5}{\overset{f_5}{=\!=}} 2H + X \qquad\qquad 7.\quad OH + X \underset{b_7}{\overset{f_7}{=\!=}} O + H + X$$

$$6.\quad H_2O + X \underset{b_6}{\overset{f_6}{=\!=}} OH + H + X \qquad\qquad 8.\quad O_2 + X \underset{b_8}{\overset{f_8}{=\!=}} 2\,O + X \qquad (1)$$

where X is a catalyst. The six active species H, O, H_2O, OH, O_2, H_2 and the inert species N_2 considered are numbered respectively from 1 to 7. The corresponding reaction rate coefficients were estimated as follows:

$$f_1 = 3 \times 10^{14} e^{-8810/T} \qquad b_1 = 2.48 \times 10^{13} e^{-660/T}$$

$$f_2 = 3 \times 10^{14} e^{-4030/T} \qquad b_2 = 1.30 \times 10^{14} e^{-2490/T}$$

$$f_3 = 3 \times 10^{14} e^{-3020/T} \qquad b_3 = 1.33 \times 10^{15} e^{-10950/T}$$

$$f_4 = 3 \times 10^{14} e^{-3020/T} \qquad b_4 = 3.12 \times 10^{15} e^{-12510/T} \qquad (2)$$

$$f_5 = 18.5 \times 10^{19} T^{-1} e^{-54000/T} \qquad b_5 = 10^{16}$$

$$f_6 = 9.66 \times 10^{21} T^{-1} e^{-62200/T} \qquad b_6 = 10^{17}$$

$$f_7 = 8.0 \times 10^{19} T^{-1} e^{-52200/T} \qquad b_7 = 10^{16}$$

$$f_8 = 5.8 \times 10^{19} T^{-1} e^{-60600/T} \qquad b_8 = 6 \times 10^{14}$$

where T is the absolute temperature in degrees Kelvin. The rates f_1-f_8 and b_1-b_4 are in units $m^3/kmol.s$, while b_5-b_8 are in $m^6/kmol^2.s$.

Let c_i be the concentration of species i (in $kmol/m^3$). The concentration C of the catalyst X is assumed to be approximately the sum of the concentrations of all species including N_2:

$$C = \sum_{i=1}^{7} c_i$$

Then, at any instant of time, the rate of change of the concentration of species i in reaction j, $\dot{c}_{ij}$, is:

$$\dot{c}_{11} = -f_1 c_1 c_5 + b_1 c_2 c_4 \qquad \dot{c}_{36} = -\dot{c}_{16}$$

$$\dot{c}_{12} = f_2 c_2 c_6 - b_2 c_1 c_4 \qquad \dot{c}_{41} = \dot{c}_{21} = -\dot{c}_{11}$$

$$\dot{c}_{13} = f_3 c_4 c_6 - b_3 c_1 c_3 \qquad \dot{c}_{42} = \dot{c}_{12}$$

$$\dot{c}_{15} = 2f_5 c_6 C - 2b_5 c_1^2 C \qquad \dot{c}_{43} = -\dot{c}_{13}$$

$$\dot{c}_{16} = f_6 c_3 C - b_6 c_4 c_1 C \qquad \dot{c}_{44} = -2\dot{c}_{24}$$

$$\dot{c}_{17} = f_7 c_4 C - b_7 c_1 c_2 C \qquad \dot{c}_{46} = \dot{c}_{16}$$

$$\dot{c}_{21} = -\dot{c}_{11} \qquad \dot{c}_{47} = -\dot{c}_{17} \qquad (3a)$$

$$\dot{c}_{22} = -\dot{c}_{12} \qquad \dot{c}_{51} = \dot{c}_{11}$$

$$\dot{c}_{24} = f_4 c_4^2 - b_4 c_2 c_3 \qquad \dot{c}_{58} = -\dot{c}_{28}/2$$

$$\dot{c}_{27} = \dot{c}_{17} \qquad \dot{c}_{62} = -\dot{c}_{12}$$

$$\dot{c}_{28} = 2f_8 c_5 C - 2b_8 c_2^2 C \qquad \dot{c}_{63} = -\dot{c}_{13}$$

$$\dot{c}_{33} = \dot{c}_{13} \qquad \dot{c}_{65} = -\dot{c}_{15}/2$$

$$\dot{c}_{34} = \dot{c}_{24}$$

The total rate of change of the concentration of species i due to all of the chemical reactions is:

$$\dot{c}_1 = \dot{c}_{11} + \dot{c}_{12} + \dot{c}_{13} + \dot{c}_{15} + \dot{c}_{16} + \dot{c}_{17}$$

$$\dot{c}_2 = -\dot{c}_{11} - \dot{c}_{12} + \dot{c}_{24} + \dot{c}_{17} + \dot{c}_{18}$$

$$\dot{c}_3 = \dot{c}_{13} + \dot{c}_{24} - \dot{c}_{16}$$

$$\dot{c}_4 = -\dot{c}_{11} + \dot{c}_{12} - \dot{c}_{13} - 2\dot{c}_{24} + \dot{c}_{16} - \dot{c}_{17} \qquad (3) \text{ Contd...}$$

$$\dot{c}_5 = \dot{c}_{11} - \dot{c}_{28}/2$$

$$\dot{c}_6 = -(\dot{c}_{12} + \dot{c}_{13} + \dot{c}_{15}/2) \tag{3}$$

The conservation of the number of atoms of hydrogen and oxygen (element conservation equations) are obtained respectively as linear combinations of Eq. (3)

$$\begin{aligned} \dot{c}_1 + 2\dot{c}_3 + \dot{c}_4 + 2\dot{c}_6 &= 0 \\ \dot{c}_2 + \dot{c}_3 + \dot{c}_4 + 2\dot{c}_5 &= 0 \end{aligned} \tag{4}$$

The concentration of species c_i are related to their mass fractions α_i as follows:

$$c_i = \frac{\rho\alpha_i}{M_i} \tag{5}$$

where M_i is the molecular weight of species i, and ρ the total density of the gas mixture.

The conservation equations for a complex reacting gas are (see, for example, the book by Penner, Ref. 19):

Conservation of species:

$$\rho \frac{dY_i}{dt} = \dot{c}_i; \quad i = 1, \ldots, 6 \tag{6}$$

Conservation of energy:

$$d\left(\sum_{i=1}^{7} \alpha_i h_i\right) = 0 \tag{7}$$

Equation of state:

$$p = R\rho YT \tag{8}$$

Hydrogen element conservation:

$$Y_f = Y_1 + 2Y_3 + Y_4 + 2Y_6 \tag{9}$$

Oxygen element conservation:

$$Y_x = Y_2 + Y_3 + Y_4 + 2Y_5 \tag{10}$$

where R is the universal gas constant, $Y_i = \alpha_i/M_i$, $Y = \sum_{i=1}^{7} Y_i$, and h_i is the partial specific static enthalpy of species i. We will assume that the reaction takes place at constant pressure. Using Eqs. (9) and (10) to determine Y_5 and Y_6, we can reduce the number of equations in (6) to four and, performing the differentiation in Eq. (7), we get the following set of six equations to determine the four species Y_1, Y_2, Y_3, Y_4, the total density ρ and the temperature T:

$$\frac{dY_i}{dt} = \frac{\dot{c}_i}{\rho} \qquad i = 1, \ldots, 4 \tag{11}$$

$$\frac{dT}{dt} = - \frac{\sum_{i=1}^{6} (h_i^* T) S_i}{\sum_{i=1}^{7} Y_i \, c_{p_i}^*} \tag{12}$$

$$\frac{d\rho}{dt} = - \frac{\rho}{T} \frac{dT}{dt} - \frac{\rho}{Y} \frac{dY}{dt} \tag{13}$$

where $S_i = \dot{c}_i/\rho$ and $h_i^* = h_i M_i/RT$. The nondimensional enthalpy h_i^* is calculated by the polynomials

$$h_i^* = A_{1_i} + \frac{A_{2_i}}{2} T + \frac{A_{3_i}}{3} T^2 + \frac{A_{4_i}}{4} T^3 + \frac{A_{5_i}}{5} T^4 + \frac{A_{6_i}}{T} \quad \text{if } T \leq 1000°$$

and

$$h_i^* = B_{1_i} + \frac{B_{2_i}}{2} T + \frac{B_{3_i}}{3} T^2 + \frac{B_{4_i}}{4} T^3 + \frac{B_{5_i}}{5} T^4 + \frac{B_{6_i}}{T} \quad \text{if } T > 1000°$$

The coefficients of these polynomials were fitted using the computer program given in Ref. 36. Thermodynamic properties were obtained from JANAF thermochemical tables (Ref. 20). The nondimensional specific heats $c_{p_i}^* = d(h_i^* T)/dT$.

3. FINITE-RATE CHEMISTRY COMPUTATIONS

The nonlinear coupled set of differential equations (11)-(13) are of the form

$$\frac{dx_i}{dt} = S_i(x_1, x_2, \ldots, x_6) \qquad (i = 1, \ldots, 6) \tag{14}$$

It is known (see Refs. 21, 22) that the numerical integration of these equations poses, in certain cases, a severe numerical stability problem. Numerical solutions involving the use of predictor-corrector methods or the use of the Runge-Kutta technique can be prohibitively expensive because they require excessive computing time. Several attempts have been made to overcome the difficulty by developing special numerical methods (Refs. 23-27). In the present investigation the method of Lomax and Bailey (Ref. 26) has been selected for the solution of Eqs. (11)-(13). The system of equations (14) is solved by the implicit modified Euler method:

$$x_i^{n+1} - x_i^n = \left(\frac{S_i^{n+1} + S_i^n}{2} \right) \Delta t \tag{15}$$

where n is a local reference time level. The value of S_i^{n+1} is calculated by expanding each S_i uniformly with respect to all dependent variables $x_1 = \rho$, $x_2 = T$, $x_3 = Y_1$, $x_4 = Y_2$, $x_5 = Y_3$ and $x_6 = Y_4$, in a Taylor series about the time level n and keeping the linear terms only,

$$S_i^{n+1} = S_i^n + \sum_{j=1}^{6} \left. \frac{\partial S_i}{\partial x_j} \right|^n \left(x_j^{n+1} - x_j^n \right) \qquad (i = 1, \ldots, 6) \tag{16}$$

Substituting Eq. (16) into Eq. (15) we get

$$x_i^{n+1} - x_i^n = S_i^n \Delta t + \sum_{j=1}^{6} \left(\left. \frac{\partial S_i}{\partial x_j} \right|^n \frac{\Delta t}{2} \right) \left(x_j^{n+1} - x_j^n \right) \qquad (i = 1, \ldots, 6) \tag{17}$$

or in matrix form

$$\left([I] - \frac{\Delta t}{2} [E] \right) \left(\vec{x}^{n+1} - \vec{x}^{n} \right) = \vec{S} \, \Delta t \tag{18}$$

where [I] is the unit matrix, the elements of the matrix E are $e_{ij} = \left. \partial S_i / \partial x_j \right|^n$, and the components of column vectors $\vec{x}$ and $\vec{S}$ are respectively $x_1, \ldots, x_6$ and $S_1, \ldots, S_6$. For any given set of initial data, the linear algebraic system of six equations, Eq. (18), can be solved by standard numerical techniques. The partial derivatives $\left. \partial S_i / \partial x_j \right|^n$ in the matrix E were calculated numerically.

The technique outlined above has been programmed, and test runs have been made for the static combustion of a stoichiometric hydrogen-air or hydrogen-"vitiated" air mixture for three sets of values of initial pressure and temperature of the mixture. The rate constants used are given in Eq. (2). The results are shown in Figs. 1-7.

Consider the temperature histories depicted on Fig. 7. These temperature histories are characterized by two time periods: the initial time interval, called the induction time of combustion, when the temperature remains almost constant, and a later period, called the energy release time, when the temperature increases rapidly from its initial value to the final temperature which is the adiabatic flame temperature. It is seen that under conditions of high initial temperature and relatively low pressure the second time interval dominates, while under conditions of relatively low initial temperature and high pressure the two time periods are of approximately equal duration.

The changes in composition during the intervals of time are shown in Figs. 1-6. The behaviour of the atomic hydrogen is of great thermodynamic significance because of its high species enthalpy per unit mass. During the induction period the mass fraction of H and the other intermediates O and OH increase rapidly and approach their equilibrium value. During this time molecular oxygen and hydrogen are depleted and water is formed. However, the chemical energy released by the formation of water is effectively absorbed by the atomic hydrogen so that no significant change in temperature occurs. The initial values of pressure and temperature do not seem to affect appreciably the maximum values of mass fraction, which are of the order of several percent. In the next section the present finite-rate chemistry computation will be used in the analysis of turbulent free jet hydrogen-air diffusion flames.

4. GOVERNING EQUATIONS

The governing equations for the coaxial mixing of two dissimilar gases including heat release by chemical reactions in the mixing region were derived assuming that the potential core region and the outer flow region are inert, inviscid and uniform. The idealized flow configuration under study is presented in Fig. 8. A central axisymmetric jet of hydrogen discharges into a coflowing airstream serving as the oxidant medium. For purposes of the present investigation the time-averaged conservation equations are used in a boundary layer form with turbulent Lewis number $Le_t = 1$. Assuming that turbulent mixing predominates to the extent that molecular transport becomes negligible, the governing equations in the axisymmetric x, r coordinate system take the following form:

Continuity:

$$\frac{\partial}{\partial x}(\rho u) + \frac{1}{r}\frac{\partial(r\rho v)}{\partial r} = 0$$

Axial Momentum:

$$\rho u \frac{\partial u}{\partial x} + \rho v \frac{\partial u}{\partial r} = -\frac{dp}{dx} + \frac{1}{r}\frac{\partial}{\partial r}\left(\mu_t\, r \frac{\partial u}{\partial r}\right) \qquad (19)$$

Contd...

Species Conservation:

$$\rho u \frac{\partial Y_K}{\partial x} + \rho v \frac{\partial Y_K}{\partial r} = \frac{1}{r} \frac{\partial}{\partial r} \left(\frac{\mu_t}{Sc_t} r \frac{\partial Y_K}{\partial r} \right) + \dot{c}_K(\rho, T, Y_1, Y_2, Y_3, Y_4)$$

$$(K = 1, \ldots, 4)$$

Hydrogen Element Conservation:

$$\rho u \frac{\partial Y_f}{\partial x} + \rho v \frac{\partial Y_f}{\partial r} = \frac{1}{r} \frac{\partial}{\partial r} \left(\frac{\mu_t}{Sc_t} r \frac{\partial Y_f}{\partial r} \right)$$

Energy:

$$\rho u \frac{\partial H}{\partial x} + \rho v \frac{\partial H}{\partial r} = \frac{1}{r} \frac{\partial}{\partial r} \left[\frac{\mu_t}{Pr_t} r \frac{\partial}{\partial r} (H - k) + \mu_t \left(1 - \frac{1}{Pr_t} \right) r \frac{\partial (u^2/2)}{\partial r} \right] \quad (19)$$

where all the dependent variables involved represent time-averaged flow quantities, u and v being the velocity components in the x and r directions, respectively, H the total enthalpy of the fluid element, and Pr_t and Sc_t the turbulent Prandtl and Schmidt numbers, respectively. The quantities Y_K represent mean species mass fractions divided by their molecular weights: $Y_K = \alpha_K / M_K$. In the species conservation equation, Eq. (19), it is assumed that the mean rate of production of each species, $\dot{c}_K$, equals the instantaneous rate with the mean quantities such as temperature, density, and species concentration replacing their instantaneous values. However, concentration measurements in turbulent flames with highly active reactions show that the time-average reaction rate in such flames is less than the values given by using the time-average values of the species mass fraction. This effect is due to high local fluctuations of temperature and species concentrations that may give rise to situations where the oxidizer and the fuel are not at the same place at the same time and may cause variations in the Arrhenius reaction rates, thus reducing the average reaction rate to values lower than those which would exist if the local average concentrations and temperature would prevail for the entire period. In the literature, this phenomenon is called "unmixedness". The analytical investigation of the combined effect of temperature and concentration fluctuations on the mean rate of production of species for a realistic combustion process in turbulent flows is a formidable task. Borghi (Ref. 28) has considered this problem for the simple case of a single forward bimolecular reaction $K + \nu O \rightarrow P$, where K denotes the fuel, O the oxidizer, P the reaction products and ν is the stoichiometric coefficient, assuming small temperature fluctuations. Later Borghi et al (Ref. 29) used approximate forms of probability density distributions for species production rate. Recently, Spiegler et al (Ref. 30) presented an interesting simplified model of unmixedness and applied it to the case of hydrogen-air axisymmetric diffusion flame. The results do show some improvement in the agreement of predicted concentration profiles with experimental results. A possible direct analytical approach to account for species concentration fluctuations only is presented in Appendix A.

The following initial and boundary conditions are imposed on the above parabolic partial differential equations, Eq. (19): at the initial section, x = 0, velocity, temperature (or total enthalpy), species mass

fraction profiles should be given. If possible, these initial profile shapes should be based on experimental data for the particular configuration of interest. In the absence of experimental data, suitable approximations for these profiles can usually be provided on the basis of general knowledge of two-dimensional or axisymmetric boundary-layer and channel flows. At the axis of symmetry the boundary conditions are:

$$r = 0, \quad \frac{\partial u}{\partial r} = \frac{\partial H}{\partial r} = \frac{\partial f}{\partial r} = \frac{\partial Y_K}{\partial r} = 0 \tag{20}$$

and at the outer edge of the mixing region the dependent variables should tend to their values in the outer (external) inviscid flow:

$$r \to \infty, \quad u \to u_E, \quad H \to H_E, \quad f \to f_E, \quad Y_K \to Y_{K_E} \tag{21}$$

5. THE TURBULENCE MODEL

The eddy viscosity μ_t in Eq. (19) is determined by means of two transport equations for the turbulent kinetic energy, k, and its dissipation rate, ϵ (two-equation model of turbulence) (Ref. 31). According to this model the magnitude of the eddy viscosity depends only on the local values of k, ϵ and the fluid density in the following way:

$$\mu_t \equiv C_\mu \frac{\rho k^2}{\epsilon} ; \qquad \epsilon = \frac{k^{3/2}}{\ell} \tag{22}$$

The quantities k and ϵ satisfy the following differential equations:

$$\rho u \frac{\partial k}{\partial x} + \rho v \frac{\partial k}{\partial r} = \frac{1}{r} \frac{\partial}{\partial r} \left(\frac{\mu_t}{\sigma_k} r \frac{\partial k}{\partial r} \right) + \mu_t \left(\frac{\partial u}{\partial r} \right)^2 - \rho \epsilon \tag{23}$$

$$\rho u \frac{\partial \epsilon}{\partial x} + \rho v \frac{\partial \epsilon}{\partial r} = \frac{1}{r} \frac{\partial}{\partial r} \left(\frac{\mu_t}{\sigma_\epsilon} r \frac{\partial \epsilon}{\partial r} \right) + \frac{C_1}{k} \epsilon \mu_t \left(\frac{\partial u}{\partial r} \right)^2 - \frac{C_2 \rho \epsilon^2}{k} \tag{24}$$

The values of the constants C_μ, C_1, C_2, σ_k and σ_ϵ are (see Ref. 13):

C_μ	C_1	C_2	σ_k	σ_ϵ
.09	1.43	1.92	1.0	1.3

The values of the Prandtl/Schmidt numbers are (Ref. 13):

$$Pr_t = Sc_t = 0.7 \qquad (Le_t = 1) \tag{25}$$

6. RESULTS AND DISCUSSION

The combustion model developed in Sections 2 and 3 to compute finite-rate hydrogen-air reactions, together with the ten equations (19, 23 and 24), were used to predict the free turbulent mixing and combustion of a hydrogen jet emerging into a co-axial airstream at a matched exit pressure of 1 atm. A schematic of the experimental setup of the flow configurations considered is depicted in Fig. 8. The air is preheated by partial combustion with hydrogen and the oxygen consumed is replaced. The composition in mass fractions of this "vitiated air" is given as 0.241 O_2, 0.281 H_2O, 0.478 N_2; it also contains small amounts of H, O, OH and H_2. For a more detailed description of the experimental apparatus, see Refs. 4 and 32. The numerical technique adopted is that of Ref. 13, and an improved version of the CHARNAL code (Ref. 13) developed at NASA Langley Research Center was extensively used in the solution of the problem. The chemistry and the turbulent diffusion processes are uncoupled by the following procedure, first devised by Ferri et al (Ref. 33).

Let

$$Y_K = Y_{K_D} + Y_{K_C}$$

$$T = T_D + T_C$$

Then the species conservation equation (19), may be split into the following two equations:

$$\rho u \frac{\partial Y_{K_C}}{\partial x} + \rho v \frac{\partial Y_{K_C}}{\partial y} = \rho \frac{dY_{K_C}}{dt} = \dot{c}_K \tag{26}$$

and

$$\rho u \frac{\partial Y_{K_D}}{\partial x} + \rho v \frac{\partial Y_{K_D}}{\partial y} = \frac{1}{r} \frac{\partial}{\partial r} \left(\frac{\mu_t}{Sc_t} r \frac{\partial Y_{K_D}}{\partial r} \right) \tag{27}$$

while the energy equation, (19), splits to

$$\rho u \frac{\partial H_C}{\partial x} + \rho v \frac{\partial H_C}{\partial r} = \frac{dH_C}{dt} = 0 \tag{28}$$

and

$$\rho u \frac{\partial H_D}{\partial x} + \rho v \frac{\partial H_D}{\partial r} = \frac{1}{r} \frac{\partial}{\partial r} \left[\frac{\mu_t}{Pr_t} r \frac{\partial}{\partial r} (H_D - k) + \mu_t \left(1 - \frac{1}{Pr_t} \right) r \frac{\partial (u^2/2)}{\partial r} \right] \tag{29}$$

Equations (26) and (28) pertain to a premixed flow of constant velocity and pressure with finite-rate chemistry and are similar to Eqs. (6) and (7) in Section 2, while Eqs. (27) and (29) refer to purely diffusive flows. The numerical solution is then performed as follows:

Diffusion Step:

For a given forward stepsize Δx_D, Eqs. (27) and (29) are used along with other conservation laws in Eqs. (19) and Eqs. (23) and (24) to find the solution of the purely diffusive step.

Chemistry Step:

The diffusion stepsize Δx_D is subdivided into a finite number of chemical steps, $\Delta t_C = \Delta x_D/nu$, where n is the number of subdivisions, and the diffusion solution is used as initial conditions for the chemistry step which uses Eqs. (26), (28), or equivalently, Eqs. (6)-(10) to determine, by the method presented in Section 3, the final values of the species, density and temperature. The value of n is determined by accuracy requirements for the chemistry step solution.

The quantity $Y_X = \alpha_X/M_2$, where α_X is the mass fraction of elemental oxygen, is yet to be determined. It satisfies a transport equation which is identical to the hydrogen element conservation equation, Eq. (19). With appropriate initial and boundary values the transport equation for Y_X can be solved and its value determined. However, using the identity of the transport equations for hydrogen and oxygen element conservation and introducing the nondimensional variables

$$Y_f^* = \frac{Y_f - Y_{f_E}}{Y_{f_{ic}} - Y_{f_E}}, \qquad Y_x^* = \frac{Y_x - Y_{x_E}}{Y_{x_{ic}} - Y_{x_E}} \tag{30}$$

where subscript E stands for the value of the variable at the external boundary of the mixing zone, and the subscript ic for its initial centerline value, which take identical boundary values of $\partial Y_f^*/\partial r = \partial Y_x^*/\partial r = 0$ and $Y_{f_E}^* = Y_{x_E}^* = 0$, we can obtain the same solution from the two identical transport equations for Y_f^* and Y_x^* if we assume identical initial values (subscript i) for Y_f^* and Y_x^* (same differential equations, same initial and boundary values), i.e.

$$\frac{Y_{f_i} - Y_{f_E}}{Y_{f_{ic}} - Y_{f_E}} = \frac{Y_{x_i} - Y_{x_E}}{Y_{x_{ic}} - Y_{x_E}} \tag{31}$$

In the jet mixing problem considered, $Y_{f_E} = \alpha_{f_E}/M_i$, $Y_{f_{ic}} = 1/M_1$, $Y_{x_E} = \alpha_{x_E}/M_2$, and $Y_{x_{ic}} = 0$. Hence from Eqs. (30) and (31) we have

$$Y_{x_i} = \frac{Y_{x_E}(1 - M_1 Y_{f_i})}{1 - M_1 Y_{f_E}} \tag{32}$$

It is easy to verify that the initial distributions of hydrogen and oxygen satisfy Eq. (32). Consequently, $Y_f^* = Y_x^*$ and from Eq. (30) we get

$$Y_x = \frac{Y_{x_E}(1 - M_1 Y_f)}{1 - M_1 Y_{f_E}}$$

The mass fraction of nitrogen is then obtained from the relation

$$\alpha_f + \alpha_x + \alpha_7 = 1$$

Figures 9-20 show some computed results at two downstream locations, $x/D_j = 6.7$ and 15.5, where $D_j = 9.525$ mm is the diameter of the hydrogen jet (Fig. 8). The initial profiles of the quantities described are also shown for convenience. With air diffusing into the inner regions and molecular hydrogen diffusing from the inner jet core into the outer regions, a turbulent mixing zone with chemical reactions is formed. The extent of the mixing and combustion process is indicated by the turbulence quantities profiles, and velocity, temperature and mass fraction profiles.

Distributions of some of the important variables affecting the flow development are shown in Figs. 9-12. The initial distribution of the turbulent kinetic energy is calculated on the basis of the mixing length hypothesis, the mixing length being proportional to the thickness of the hydrogen nozzle wall d = 1.57 mm (Fig. 8). The quantity d is also used as the constant initial turbulence scale (Fig. 11a). The initial distributions of the dissipation rate ϵ (Fig. 10a) and the eddy viscosity μ_t (Fig. 12a) are then calculated from Eq. (22). It is seen from these figures that far downstream (curves c) all the quantities involved tend to reach their maximum values at the axis of symmetry. As the shear flow develops downstream the mixing zone spreads and the levels of the corresponding variables fall. At the outer edge of the mixing zone the curves should tend to the same value of the corresponding variable which prevail in the outer flow. However, the computed profiles depict this trend only approximately.

Velocity and temperature profiles at the selected downstream locations are shown on Figs. 13 and 14. The wake region of the profiles (Fig. 13, curves a and b) arises from the wall boundary layers of the hydrogen pipe. Note that the potential core (see Fig. 8) is still present at $x/D_j = 6.7$. As the mixing progresses downstream, hydrogen jet and air velocities tend to equalize. At the outer edge of the mixing zone the velocity and temperature profiles tend to values prevailing in the external stream. From the temperature profiles shown in Fig. 14 the region of combustion is clearly evident through the peak in the temperature level. It can be seen that the increase in the maximum temperature values becomes less appreciable as the mixing process develops downstream. No temperature increase is observed at the centreline with a distance 6-7 diameters from the origin.

As a result of the combustion process, chemical species are formed. The calculated distributions of atomic species H and O of the hydroxyl radical, OH, and water, H_2O, are shown in Figs. 15-18. It can readily be seen that the peak values reached by these species at some distance downstream remain approximately constant or decay, and as the shear flow develops and the jet spreads, shift toward the outer region of the flow. The maximum computed value of OH at $x/D_j = 15.5$ is $\sim 2\%$ by mass, and is about ten times as large as the maximum mass fraction of H and approximately three and a half times as large as the peak mass fraction of O. Within the computed distances, traces of H are present at the centreline, whereas the mass fractions of O and OH are still very small at the axis. The mass fraction profile of the most important combustion product H_2O displays peaks in the inner region of the flame where the exothermic reactions are most intense. Traces of H_2O are observed at the centreline only after $x/D_j \gtrsim 2$. All profiles tend to their values in the outer region of the flow.

O_2 distributions are primarily determined by the diffusion-controlled mixing process, but as chemical reactions become important in the turbulent mixing layer, the interaction between the diffusional process and the chemical reactions become very complicated, as indicated by the peaks and minima in the predicted profiles in Fig. 19. The mass fraction distribution of molecular hydrogen is depicted in Fig. 20.

To account for the effects of species concentration fluctuations on the mean production rate of species (the unmixedness), the analytical approach developed in Appendix A was programmed and the subroutine incorporated into the main computer program. Local equilibrium turbulence was assumed (production of turbulence and its dissipation rate balance each other, i.e. $C_{g_1} = C_{g_2} = 0$ in Eq. (A13)). In view of the excessively large amount of computer time required to solve the system of twenty-four differential equations with finite-rate chemistry (70 min on CDC 7600 for a distance $x/D_j = 5$) further computations with this method did not seem justified. Comparison of species mass fractions at $x/D_j = 8.2$ without unmixedness and with it, revealed no appreciable differences in the predicted values of species at these distances.

Analytical predictions were compared to experimental data obtained by Cohen and Guile (Ref. 4) and Evans, Schexnayder and Beach (Ref. 35). Detailed descriptions of the experimental apparatus, instrumentation and experimental procedures are given in these references and in Ref. 32. The initial velocity and temperature profiles for the two cases considered are shown in Fig. 21. The initial mass fractions of species in the outer vitiated air flow are: for the Cohen and Guile case, 0.26 O_2, 0.15 H_2O, 0.59 N_2, and for the Beach case (Ref. 35), 0.241 O_2, 0.281 H_2O, 0.478 N_2. Both cases contained also small amounts of H, O, OH and H_2.

The computed and experimental pitot pressure profiles at axial distances 5.2 and 8.9 jet diameters for the Cohen and Guile case and at 6.56 jet diameter for the Beach case are shown in Figs. 23 and 24. In the Beach case the theory predicts the minimum pitot pressure and the general trend of the spread of the mixing region relatively well. In both cases and at all distances, theoretically predicted spread of the mixing region is larger than that given by experimental data. However, it is readily seen that the slopes of predicted and experimental profiles are almost identical. The discrepancy is primarily due to the differences in the predicted and experimental minimum values of the pitot pressure. Species mass fractions are compared to data in Figs. 24-26. In both cases and at all distances the agreement for the inert species N_2 is good. Quantitative agreement for hydrogen improves with downstream distance. The agreement for oxygen is better in Beach's case. In both cases a small amount of oxygen is present in the hydrogen-rich region near the axis of symmetry. This is due to the diffusion of oxygen into the hydrogen region in the gap between the lip of the hydrogen nozzle and the point where the flame is initiated. Figure 26 shows that in both cases the predicted water profile bumps are not placed according to data. Again, relatively better agreement is achieved in Beach's case.

7. CONCLUSIONS

By using a two-equation (k-ϵ) model of turbulence and a finite-rate chemistry model, an analytical-numerical investigation was made of the turbulent mixing and combustion of a round hydrogen jet in a parallel ambient coflowing air stream. Theoretical calculations were unable to correctly predict experimental results. An attempt was made to account for the species concentration fluctuations on the mean-production rate of these species (the phenomenon of unmixedness). Comparisons of species mass fractions without unmixedness and with it, assuming that local equilibrium turbulence prevails in the flow field, revealed no appreciable differences in the predicted values of species mass fractions. Improved experimental data, more accurate determination of initial conditions, preferably given by the solution of the full Navier-Stokes equation in the near flow field, and proper account of the phenomenon of unmixedness and compressibility effects, could considerably decrease the discrepancy between predicted and experimental values.

APPENDIX A

DERIVATION OF THE DIFFERENTIAL EQUATIONS FOR THE TRANSPORT OF SECOND-ORDER CORRELATIONS OF SPECIES CONCENTRATION FLUCTUATIONS

1. Species Production Rate in Turbulent Flow

Let Y_K be split, in conventional fashion, into time-average parts $\bar{Y}_K$ and fluctuating part Y'_K. Thus

$$Y_K = \bar{Y}_K + Y'_K \tag{A1}$$

Then, substituting expressions (5) and (A1) into the rate of change of the concentration of species i in reaction j, given by Eq. (3a), and taking the average, we obtain the following expressions (temperature fluctuations are neglected):

$$\begin{aligned}
\bar{\dot{c}}_{11} &= \rho^2[-f_1(\bar{Y}_1\bar{Y}_5 + Z_{15}) + b_1(\bar{Y}_2\bar{Y}_4 + Z_{24})] \\
\bar{\dot{c}}_{12} &= \rho^2[f_2(\bar{Y}_2\bar{Y}_6 + Z_{26}) - b_2(\bar{Y}_1\bar{Y}_4 + Z_{14})] \\
\bar{\dot{c}}_{13} &= \rho^2[f_3(\bar{Y}_4\bar{Y}_6 + Z_{46}) - b_3(\bar{Y}_1\bar{Y}_3 + Z_{13})] \\
\bar{\dot{c}}_{15} &= \rho^2[2f_5(\bar{Y}_6\bar{Y} + Z_6)] - \rho^3[2b_5(\bar{Y}_1{}^2\bar{Y} + \bar{Y}Z_{11} + 2\bar{Y}_1Z_1)] \\
\bar{\dot{c}}_{16} &= \rho^2[f_6(\bar{Y}_3\bar{Y} + Z_3)] - \rho^3[b_6(\bar{Y}_4\bar{Y}_1\bar{Y} + \bar{Y}Z_{14} + \bar{Y}_1Z_4 + \bar{Y}_4Z_1)] \\
\bar{\dot{c}}_{17} &= \rho^2[f_7(\bar{Y}\,\bar{Y}_4 + Z_4)] - \rho^3[b_7(\bar{Y}_1\bar{Y}_2\bar{Y} + \bar{Y}Z_{12} + \bar{Y}_2Z_1 + \bar{Y}_1Z_2)] \\
\bar{\dot{c}}_{24} &= \rho^2[f_4(\bar{Y}_4{}^2 + Z_{44}) - b_4(\bar{Y}_2\bar{Y}_3 + Z_{23})] \\
\bar{\dot{c}}_{28} &= \rho^2[2f_8(\bar{Y}\,\bar{Y}_5 + Z_5)] - \rho^3[2b_8(\bar{Y}\,\bar{Y}_2{}^2 + \bar{Y}\,Z_{22} + 2\bar{Y}_2Z_2)]
\end{aligned} \tag{A2}$$

where

$$Z_{\alpha\beta} = \overline{Y'_\alpha\, Y'_\beta}, \qquad Z_K = \overline{Y'Y'_K} = \sum_{i=1}^{7} Z_{iK} \qquad (\alpha, \beta, K = 1, \ldots, 7) \tag{A3}$$

and

$$\rho^2 = \left(\frac{\bar{p}}{R\tilde{Y}\tilde{T}} \right)^2$$

from the equation of state, Eq. (8), assuming that

$$\sum_{i=1}^{7} Y_i' \approx 0$$

Hence, in Eq. (A2) we have the following set of unknown second-order correlations of species mole-mass fraction fluctuations:

$$\begin{array}{ccccc:ccc} Z_{11} & Z_{12} & Z_{13} & Z_{14} & Z_{15} & Z_{16} & Z_{17} \\ & Z_{22} & Z_{23} & Z_{24} & Z_{25} & Z_{26} & Z_{27} \\ & & Z_{33} & Z_{34} & Z_{35} & Z_{36} & Z_{37} \\ & & & Z_{44} & Z_{45} & Z_{46} & Z_{47} \\ & & & & Z_{55} & Z_{56} & Z_{57} \\ & & & & & Z_{66} & Z_{67} \end{array} \qquad \text{(A4)}$$

In the next section it will be shown that the following 15 independent quantities

$$\begin{array}{ccccc} Z_{ff} & Z_{f1} & Z_{f2} & Z_{f3} & Z_{f4} \\ & Z_{11} & Z_{12} & Z_{13} & Z_{14} \\ & & Z_{22} & Z_{23} & Z_{24} \\ & & & Z_{33} & Z_{34} \\ & & & & Z_{44} \end{array} \qquad \text{(A5)}$$

can be determined from 15 transport equations derived by using the four species conservation equations and the hydrogen element conservation equations for the instantaneous flow. The quantities on the right-hand side of the dotted line

in Eq. (A4) are functions of quantities in Eq. (A5) and can be determined by using the hydrogen and oxygen element conservation equations, Eqs. (9) and (10), in the following way: From Eqs. (9), (10), (32), (33) and (A1) we get:

$$\begin{aligned}
\bar{Y}_x &= \varphi(1 - M_1\bar{Y}_f) \\
\bar{Y}_5 &= (\bar{Y}_x - \bar{Y}_2 - \bar{Y}_3 - \bar{Y}_4)/2 \\
\bar{Y}_6 &= (\bar{Y}_f - \bar{Y}_1 - 2\bar{Y}_3 - \bar{Y}_4)/2 \\
\bar{Y}_7 &= (1 - \varphi)(1 - M_1\bar{Y}_f)/M_7
\end{aligned} \tag{A6}$$

for the mean values, and

$$\begin{aligned}
Y'_x &= - \varphi M_1 Y'_f = CY'_f \\
Y'_5 &= (Y'_x - Y'_2 - Y'_3 - Y'_4)/2 \\
Y'_6 &= (Y'_f - Y'_1 - 2Y'_3 - Y'_4)/2 \\
Y'_7 &= - (1 - \varphi)M_1 Y'_f/M_7 = BY'_f
\end{aligned} \tag{A7}$$

for the fluctuating parts. Multiplying Y'_5, Y'_6, Y'_7 successively by Y'_f, Y'_1, Y'_2, Y'_3, Y'_4, Y'_5, Y'_6 and Y'_7 and taking the average we get:

$$\begin{aligned}
Z_{f5} &= (CZ_{ff} - Z_{f2} - Z_{f3} - Z_{f4})/2 \\
Z_{f6} &= (Z_{ff} - Z_{f1} - 2Z_{f3} - Z_{f4})/2 \\
Z_{f7} &= BZ_{ff} \\
Z_{15} &= (CZ_{f1} - Z_{12} - Z_{13} - Z_{14})/2 \\
Z_{25} &= (CZ_{f2} - Z_{22} - Z_{23} - Z_{24})/2 \\
Z_{35} &= (CZ_{f3} - Z_{23} - Z_{33} - Z_{34})/2
\end{aligned} \tag{A8}$$

Contd...

$$Z_{45} = (CZ_{f4} - Z_{24} - Z_{34} - Z_{44})/2$$

$$Z_{55} = (C^2 Z_{ff} + Z_{22} + Z_{33} + Z_{44} - 2CZ_{f2} - 2CZ_{f3} -$$

$$- 2CZ_{f4} + 2Z_{23} + 2Z_{24} + 2Z_{34})/4$$

$$Z_{16} = (Z_{f1} - Z_{11} - 2Z_{13} - Z_{14})/2$$

$$Z_{26} = (Z_{f2} - Z_{12} - 2Z_{23} - Z_{24})/2$$

$$Z_{36} = (Z_{f3} - Z_{13} - 2Z_{33} - Z_{34})/2$$

$$Z_{46} = (Z_{f4} - Z_{14} - 2Z_{34} - Z_{44})/2$$

$$Z_{56} = [CZ_{ff} - Z_{f2} - (2C + 1)Z_{f3} - (C + 1)Z_{f4} - CZ_{f1} +$$

$$+ Z_{12} + Z_{13} + Z_{14} + 2Z_{23} + 2Z_{33} + Z_{24} + 3Z_{34} + Z_{44}]/4$$

$$Z_{66} = (Z_{ff} + Z_{11} + 4Z_{33} + Z_{44} - 2Z_{f1} - 4Z_{f3} - 2Z_{f4} +$$

$$+ 4Z_{13} + 2Z_{14} + 4Z_{34})/4$$

$$Z_{17} = BZ_{f1};\ Z_{27} = BZ_{f2};\ Z_{37} = BZ_{f3};\ Z_{47} = BZ_{f4}$$

$$Z_{57} = (CZ_{f7} - Z_{27} - Z_{37} - Z_{47})/2$$

$$Z_{67} = (Z_{f7} - Z_{17} - 2Z_{37} - Z_{47})/2 \qquad \text{(A8)}$$

2. Equation for the Transport of the Second-Order Species Concentration Fluctuations

The species and element conservation laws for the instantaneous flow can be expressed by the following single equation:

$$\frac{\partial}{\partial x}(\rho u Y_\alpha) + \frac{1}{r}\frac{\partial}{\partial r}(r\rho v Y_\alpha) = \frac{1}{r}\frac{\partial}{\partial r}\left(r\,\frac{\mu}{Sc}\,\frac{\partial Y_\alpha}{\partial r}\right) + \dot{c}_\alpha \left[\frac{\text{kmol of } \alpha}{m^3\ s}\right] \qquad \text{(A9)}$$

where the subscript α denotes any element (in that case $\dot{c}_\alpha = 0$) or species present. Decomposing the dependent variables in Eq. (A9) into their time-

average and fluctuation parts, multiplying by Y'_β and using the continuity equation for the mean and fluctuating parts, after some transformations we get:

$$(\rho u)' Y'_\beta \frac{\partial \bar{Y}_\alpha}{\partial x} + \overline{\rho u} Y'_\beta \frac{\partial Y'_\alpha}{\partial x} + (\rho u)' Y'_\beta \frac{\partial Y'_\alpha}{\partial x} + Y'_\alpha Y'_\beta \frac{\partial (\rho u)'}{\partial x} +$$

$$+ (\rho v)' Y'_\beta \frac{\partial \bar{Y}_\alpha}{\partial r} + \overline{\rho v} Y'_\beta \frac{\partial Y'_\alpha}{\partial r} + \frac{Y'_\beta}{r} \frac{\partial}{\partial r} [r(\rho v)' Y'_\alpha] = \frac{Y'_\beta}{r} \frac{\partial}{\partial r} \left[r \frac{\mu}{Sc} \frac{\partial \bar{Y}_\alpha}{\partial r} \right] +$$

$$+ \frac{1}{r} \frac{\partial}{\partial r} \left[r \frac{\mu}{Sc} Y'_\beta \frac{\partial Y'_\alpha}{\partial r} \right] - \frac{\mu}{Sc} \frac{\partial Y'_\alpha}{\partial r} \cdot \frac{\partial Y'_\beta}{\partial r} + Y'_\beta \dot{\bar{c}}_\alpha + Y'_\beta \dot{c}'_\alpha \qquad (A10)$$

Interchanging α and β and adding the resulting expression to Eq. (10) we obtain:

$$\overline{\rho u} \frac{\partial Y'_\alpha Y'_\beta}{\partial x} + \overline{\rho v} \frac{\partial Y'_\alpha Y'_\beta}{\partial r} + (\rho u)' Y'_\beta \frac{\partial \bar{Y}_\alpha}{\partial x} + (\rho u)' Y'_\alpha \frac{\partial \bar{Y}_\beta}{\partial x} + \frac{\partial}{\partial x} [(\rho u)' Y'_\alpha Y'_\beta] =$$

$$= \frac{Y'_\beta}{r} \frac{\partial}{\partial r} \left[r \frac{\mu}{Sc} \frac{\partial Y_\alpha}{\partial r} \right] + \frac{Y'_\alpha}{r} \frac{\partial}{\partial r} \left[r \frac{\mu}{Sc} \frac{\partial \bar{Y}_\beta}{\partial r} \right] + \frac{1}{r} \frac{\partial}{\partial r} \left[r \frac{\mu}{Sc} \frac{\partial Y'_\alpha Y'_\beta}{\partial r} \right] -$$

$$- \frac{1}{r} \frac{\partial}{\partial r} [r(\rho v)' Y'_\alpha Y'_\beta] - (\rho v)' Y'_\beta \frac{\partial \bar{Y}_\alpha}{\partial r} - (\rho v)' Y'_\alpha \frac{\partial \bar{Y}_\beta}{\partial r} - 2 \frac{\mu}{Sc} \frac{\partial Y'_\alpha}{\partial r} \frac{\partial Y'_\beta}{\partial r} + \qquad (A11)$$

$$+ Y'_\beta \dot{\bar{c}}_\alpha + Y'_\alpha \dot{\bar{c}}_\beta + Y'_\beta \dot{c}'_\alpha + Y'_\alpha \dot{c}'_\beta$$

Neglecting the turbulent diffusion terms $(\rho u)' Y'_\beta$ and $(\rho u)' Y'_\alpha$ in the x-direction (in the boundary layer approximation) and the third-order correlations, and averaging we get:

$$\overline{\rho u} \frac{\partial Y'_\alpha Y'_\beta}{\partial x} + \overline{\rho v} \frac{\partial Y'_\alpha Y'_\beta}{\partial r} = \frac{1}{r} \frac{\partial}{\partial r} \left[r \frac{\mu}{Sc} \frac{\partial Y'_\alpha Y'_\beta}{\partial r} - (\rho v)' Y'_\alpha Y'_\beta \right] -$$

$$- (\rho v)' Y'_\beta \frac{\partial Y_\alpha}{\partial r} - (\rho v)' Y'_\alpha \frac{\partial Y_\beta}{\partial r} - 2 \frac{\mu}{Sc} \frac{\partial Y'_\alpha}{\partial r} \frac{\partial Y'_\beta}{\partial r} + Y'_\beta \dot{c}'_\alpha + Y'_\alpha \dot{c}'_\beta \qquad (A12)$$

Using the approximations

$$-(\rho v)' Y'_\alpha Y'_\beta = \frac{\mu_t}{Sc_t} \frac{\partial Y'_\alpha Y'_\beta}{\partial r}; \qquad -(\rho v)' Y'_\beta = \frac{\mu_t}{Sc_t} \frac{\partial \bar{Y}_\beta}{\partial r}; \qquad -(\rho v)' Y'_\alpha = \frac{\mu_t}{Sc_t} \frac{\partial \bar{Y}_\alpha}{\partial r}$$

and modelling the dissipation term (see Ref. 34) by:

$$2\,\frac{\mu}{Sc}\,\frac{\partial Y'_\alpha}{\partial r}\,\frac{\partial Y'_\beta}{\partial r} = C_{g_2}\,\frac{\rho\epsilon}{k}\,Y'_\alpha Y'_\beta$$

and using Eq. (A3) we finally obtain the transport equations for the quantities $Z_{\alpha\beta}$:

$$\overline{\rho u}\,\frac{\partial Z_{\alpha\beta}}{\partial x} + \overline{\rho v}\,\frac{\partial Z_{\alpha\beta}}{\partial r} = \frac{1}{r}\,\frac{\partial}{\partial r}\left[\, r\left(\frac{\mu}{Sc} + \frac{\mu_t}{Sc_t}\right)\frac{\partial Z_{\alpha\beta}}{\partial r}\,\right] +$$

$$+ C_{g_1}\,\mu_t\,\frac{\partial \bar{Y}_\alpha}{\partial r}\cdot\frac{\partial \bar{Y}_\beta}{\partial r} - C_{g_2}\,\frac{\rho\epsilon}{k}\,Z_{\alpha\beta} + Y'_\beta\,\dot{c}'_\alpha + Y'_\alpha\,\dot{c}'_\beta \qquad \text{(A13)}$$

where $C_{g1} = 2/Sc_t$. For the case considered in the present study, α, β take the values of f (for the hydrogen element), 1, 2, 3, 4 for H, O, H_2O and OH, respectively Hence, Eq (A13) constitutes a system of 15 equations for the 15 unknown quantities represented in Eq. (A5). It is assumed that the turbulent Schmidt number $Sc_t = 0.7$ and the constant $C_{g2} = 2.0$ (Ref 34) in all the 15 equations. The last two terms on the right-hand side of Eq. (A13) can be calculated by developing the $\dot{c}_{ij}$ given in Eq. (3a) into their mean and fluctuating parts:

$$\bar{\dot{c}}_{11} + \dot{c}'_{11} = \rho^2[-f_1(\bar{Y}_1\bar{Y}_5 + Y'_1\bar{Y}_5 + Y'_5\bar{Y}_1 + Y'_1Y'_5) + b_1(\bar{Y}_2\bar{Y}_4 + Y'_2\bar{Y}_4 + Y'_4\bar{Y}_2 + Y'_2Y'_4)]$$

$$\bar{\dot{c}}_{12} + \dot{c}'_{12} = \rho^2[f_2(\bar{Y}_2\bar{Y}_6 + Y'_2\bar{Y}_6 + Y'_6\bar{Y}_2 + Y'_2Y'_6) - b_2(\bar{Y}_1\bar{Y}_4 + Y'_1\bar{Y}_4 + Y'_4\bar{Y}_1 + Y'_1Y'_4)]$$

$$\bar{\dot{c}}_{13} + \dot{c}'_{13} = \rho^2[f_3(\bar{Y}_4\bar{Y}_6 + Y'_4\bar{Y}_6 + Y'_6\bar{Y}_4 + Y'_4Y'_6) - b_3(\bar{Y}_1\bar{Y}_3 + Y'_1\bar{Y}_3 + Y'_3\bar{Y}_1 + Y'_1Y'_3)]$$

$$\bar{\dot{c}}_{15} + c'_{15} = \rho^2[2f_5(\bar{Y}_6\bar{Y} + Y'_6\bar{Y} + Y'\bar{Y}_6 + Y'Y'_6)] - \rho^3[2b_5(\bar{Y}_1{}^2\bar{Y} + 2\bar{Y}_1\bar{Y}Y'_1 + \bar{Y}Y'_1{}^2 +$$

$$+ \bar{Y}_1{}^2Y' + 2\bar{Y}_1Y'_1Y' + Y'_1{}^2Y')]$$

$$\bar{\dot{c}}_{16} + \dot{c}'_{16} = \rho^2[f_6(\bar{Y}_3\bar{Y} + \bar{Y}Y'_3 + \bar{Y}_3Y' + Y'Y'_3)] - \rho^3[b_6(\bar{Y}_4\bar{Y}_1\bar{Y} + \bar{Y}_1\bar{Y}Y'_4 + \bar{Y}\bar{Y}_4Y'_1 +$$

$$+ \bar{Y}Y'_1Y'_4 + \bar{Y}_4\bar{Y}_1Y' + \bar{Y}_1Y'Y'_4 + \bar{Y}_4Y'Y'_1 + Y'_1Y'_4Y')]$$

$$\bar{\dot{c}}_{17} + \dot{c}'_{17} = \rho^2[f_7(\bar{Y}\bar{Y}_4 + \bar{Y}Y'_4 + Y'\bar{Y}_4 + Y'Y'_4)] - \rho^3[b_7(\bar{Y}_1\bar{Y}_2\bar{Y} + \bar{Y}_2\bar{Y}Y'_1 + \bar{Y}\bar{Y}_1Y'_2 +$$

$$+ \bar{Y}Y'_1Y'_2 + \bar{Y}_1\bar{Y}_2Y' + \bar{Y}_2Y'_1Y' + \bar{Y}_1Y'_2Y' + Y'_1Y'_2Y')]$$

$$\bar{\dot{c}}_{24} + \dot{c}'_{24} = \rho^2[f_4(\bar{Y}_4{}^2 + 2Y_4Y'_4 + Y'_4{}^2) - b_4(\bar{Y}_2\bar{Y}_3 + Y'_2\bar{Y}_3 + Y'_3\bar{Y}_2 + Y'_2Y'_3)]$$

$$\bar{\dot{c}}_{28} + \dot{c}'_{28} = \rho^2[2f_8(\bar{Y}\bar{Y}_5 + \bar{Y}Y'_5 + Y'\bar{Y}_5 + Y'Y'_5)] - \rho^3[2b_8(\bar{Y}\bar{Y}_2^2 + 2\bar{Y}_2\bar{Y}Y'_2 + \bar{Y}Y'^2_2 +$$

$$+ \bar{Y}_2^2Y' + 2\bar{Y}_2Y'_2Y' + Y'^2_2Y')]$$

using Eq. (3), multiplying the corresponding $\bar{\dot{c}}_\alpha + \dot{c}'_\alpha$ by Y'_β and $\bar{\dot{c}}_\beta + \dot{c}'_\beta$ by Y'_α, taking the average and neglecting third and higher order correlations. The resulting expressions will then be functions of ρ, f_1, ..., f_8, b_1, ..., b_8, $\bar{Y}_i$ and $Z_{\alpha\beta}$, and being cumbersome are not reported here. Their derivation is straightforward.

REFERENCES

1. Ferri, A., Libby, P. A., Zakkay, V. — Theoretical and Experimental Investigation of Supersonic Combustion, in High Temperatures in Aeronautics. 1962, pp. 55-118, Pergamon Press, New York.

2. Libby, P. A. — Theoretical Analysis of Turbulent Mixing of Reactive Gases with Application to Supersonic Combustion of Hydrogen. J. Amer. Rocket Soc., 1962, 32, pp. 388-395.

3. Zakkay, V., Krause, E. — Mixing Problems with Chemical Reactions, in Supersonic Flow, Chemical Processes and Radiative Transfer. 1964, pp. 3-29, Pergamon Press, New York.

4. Cohen, L. S., Guile, R. N. — Investigation of the Mixing and Combustion of Turbulent, Compressible Free Jets. NASA CR-1473, 1969, 100 pp.

5. Bray, K.N.C., Fletcher, A. S., Murad, R. J. — Studies of Turbulent Mixing and Combustion in Supersonic Heterogeneous Flows. AFOSR TR-71-1915, 1971, 39 pp.

6. Leuchter, O. — Etude des Evolutions Chimiques dans une Couche de Melange Hydrogene-Air. ONERA T. P. No. 981; English Translation: NASA TTF-14633.

7. Wang, R. L. — Non-Equilibrium Turbulent Free Jet Mixing of Compressible Reacting Gases. Astronautica Acta, 1973, 18, pp. 367-382.

8. Baev, V. K., Golovichev, V. I., Dimitrov, V. I., Yasakov, V. A. — Calculation of Ignition and Combustion of a Hydrogen Jet in Air with Finite Chemical Reaction Rates. Astronautica Acta, 1974, 1, pp. 1227-1238.

9. Drewry, J. E. — Supersonic Mixing and Combustion of Coaxial Hydrogen-Air Streams in a Duct. ARL Report 71-0286.

10. Jensen, D. E., Wilson, A. S. — Prediction of Rocket Exhaust Flame Properties. Combustion and Flame. 1975, 25, pp. 43-55.

11. Oyegbesan, A. O., Algermissen, J. — Numerical Analysis of a Nonequilibrium Turbulent Free Jet Diffusion Flame. Astronautica Acta, 1976, 3, pp. 281-292.

12. Thomas, P. D., Wilson, K. H. — Efficient Computation of "Stiff" Chemically Reacting Flow in Turbulent Free Jets. AIAA J., 1976, 14, No. 5, pp. 629-636.

13. Spalding, D. B.; Launder, B. E.; Morse, A. P.; Maples, G. — Combustion of Hydrogen-Air Jets in Local Chemical Equilibrium (A Guide to CHARNAL Computer Program). NASA CR-2407, 1974.

14. Duff, R. E. — Calculation of Reaction Profiles Behind Steady-State Shock Waves. I. Application to Detonation Waves. J. Chem. Phys., 1958, 28, No. 6, pp. 1193-1197.

15. Schott, G. L.; Kinsey, J. L. — Kinetic Studies of Hydroxyl Radicals in Shock Waves. II. Induction Times in the Hydrogen-Oxygen Reaction. J. Chem. Phys., 1958, 29, No. 5, pp. 1177-1182.

16. Schott, G. L. — Kinetic Studies of Hydroxyl Radicals in Shock Waves. III. The OH Concentration Maximum in the Hydrogen-Oxygen Reaction. J. Chem. Phys., 1960, 32, No. 3, pp. 710-716.

17. Momtchiloff, I. N.; Taback, E. D.; Buswell, R. F. — An Analytical Method of Computing Reaction Rates for Hydrogen-Air Mixtures. 9th Internat. Symp. Combustion, Cornell Univ., Ithaca, New York, August 1962.

18. Pergament, H. S. — A Theoretical Analysis of Nonequilibrium Hydrogen-Air Reactions in Flow Systems. AIAA Paper No. 6-113, 1963.

19. Penner, S. S. — Chemistry Problems in Jet Propulsion. Pergamon Press, 1957.

20. Anon. — JANAF Thermochemical Tables. Dow Chemical Co., 1969.

21. Curtiss, C. F.; Hirschfelder, J. O. — Integration of Stiff Equations. Proc. Natl. Acad. Sci., U.S.A., 1952, 38, pp. 235-243.

22. Emanuel, G. — Problems Underlying the Numerical Integration of the Chemical and Vibrational Rate Equations in a Near Equilibrium Flow. AEDC-TDR-63-82, Arnold Engineering Development Center, Tullahoma, Tenn., 1963.

23. Moretti, G. — A New Technique for the Numerical Analysis of Nonequilibrium Flows. AIAA J., 1965, 3, No. 2, pp. 223-229.

24. Tyson, T. J. — An Implicit Integration Method for Chemical Kinetics. TRW Space Technology Lab. Rep. 9840-6002-RU000, Sept. 1964.

25. Treanor, C. E. — A Method for the Numerical Integration of Coupled First-Order Differential Equations with Greatly Different Time Constants. Math. Comp., 1966, 20, No. 93, pp. 39-45.

26. Lomax, H.
Bailey, H. E.
A Critical Analysis of Various Numerical Integration Methods for Computing the Flow of a Gas in Chemical Nonequilibrium. NASA TN D-4109, 1967.

27. McLain, A. G.
Rao, C.S.R.
A Hybrid Computer Program for Rapidly Solving Flowing or Static Chemical Kinetic Problems Involving Many Chemical Species. NASA TM X-3403, 1976.

28. Borghi, R.
Computational Studies of Turbulent Flows with Chemical Reaction. ONERA TN-1383, 1974.

29. Borghi, R.
Moreau, P.
Bonniot, C.
Theoretical Predictions of a High Velocity Premixed, Turbulent Flame. ONERA TN-1977-66.

30. Spiegler, E.
Wolfshtein, M.
Manheimer-Timnat, Y.
Model of Unmixedness for Turbulent Reacting Flows. Astronautica Acta, 1966, 3, pp. 265-280.

31. Launder, B. E.
Morse, A.
Spalding, D. B.
Rodi, W.
Prediction of Free Shear Flows - A Comparison of the Performance of Six Turbulence Models. Proc. of Free Shear Flows Conference, 1972, NASA SP 321.

32. Beach, H. L., Jr.
A Study of Reacting Free and Ducted Hydrogen/Air Jets. NASA TM X-72678.

33. Ferri, A.
Moretti, G.
Slutsky, S.
Mixing Processes in Supersonic Combustion. J. Soc. Industr. Appl. Math., 1965, 13, No. 1, pp. 229-258.

34. Spalding, D. B.
Concentration Fluctuations in a Round Turbulent Jet. Chemical Engng. Sci., 1971, 26, pp. 95-107.

35. Evans, John S.
Schexnayder, Charles J., Jr.
Beach, H. L., Jr.
Application of a Two-Dimensional Parabolic Computer Program to the Prediction of Turbulent Reacting Flows. NASA TP 1169, 1978.

36. Zelesnik, F. J.
Gordon, S.
A General IBM 704 or 7090 Computer Program for Computation of Chemical Equilibrium Composition, Rocket Performance and Chapman-Jouguet Detonations. NASA TN D-1454, 1962.

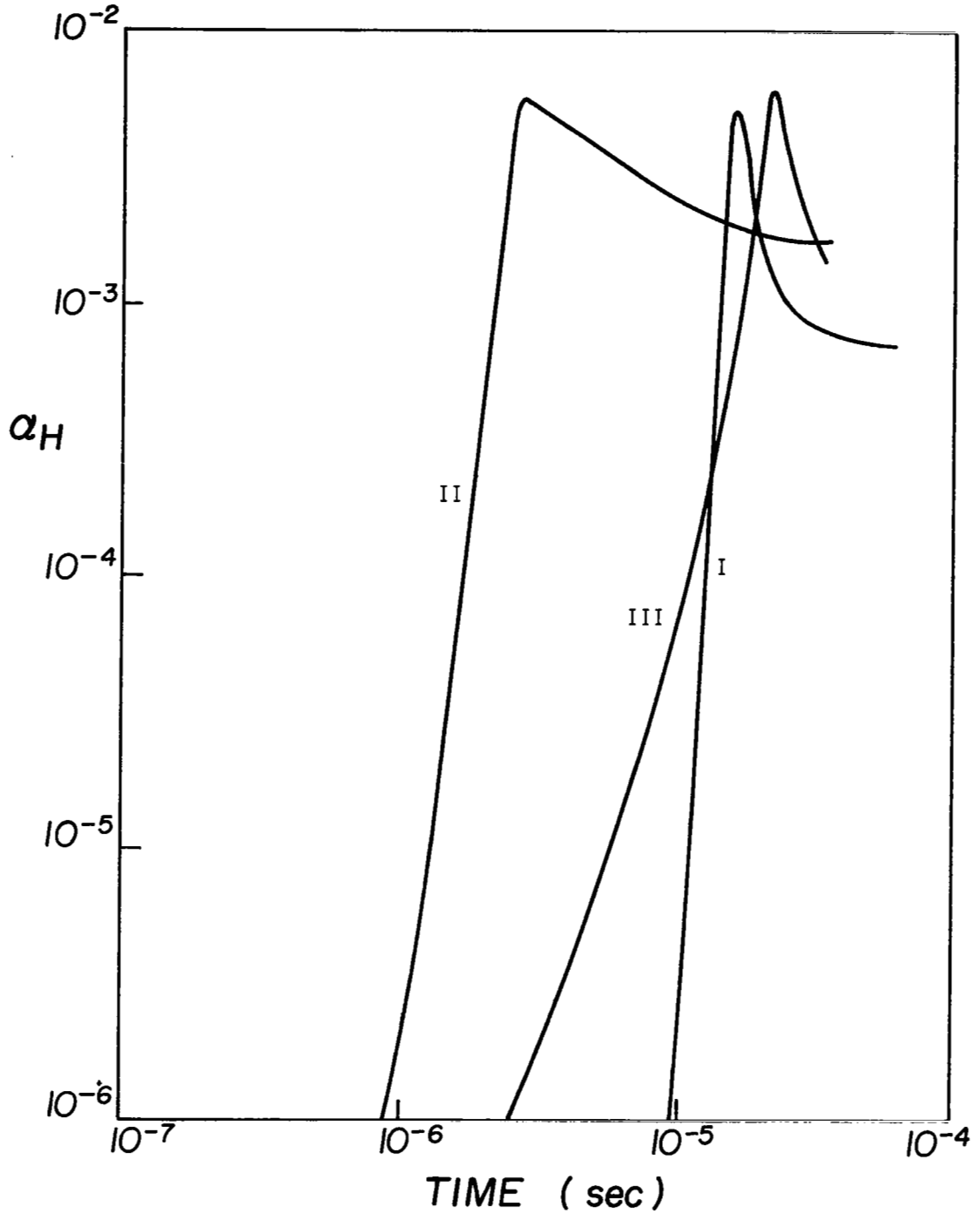

FIG. 1 VARIATION OF MASS FRACTION OF ATOMIC HYDROGEN α_H IN STOICHIOMETRIC HYDROGEN-AIR MIXTURES AT CONSTANT PRESSURE.

CURVE I: P = 1.51 atm, T = 1340°K
CURVE II: P = 1 atm, T = 2000°K
CURVE III: P = 1 atm, T = 1140°K, Vitiated Air $\alpha_{H_2O\ init} = 0.15$

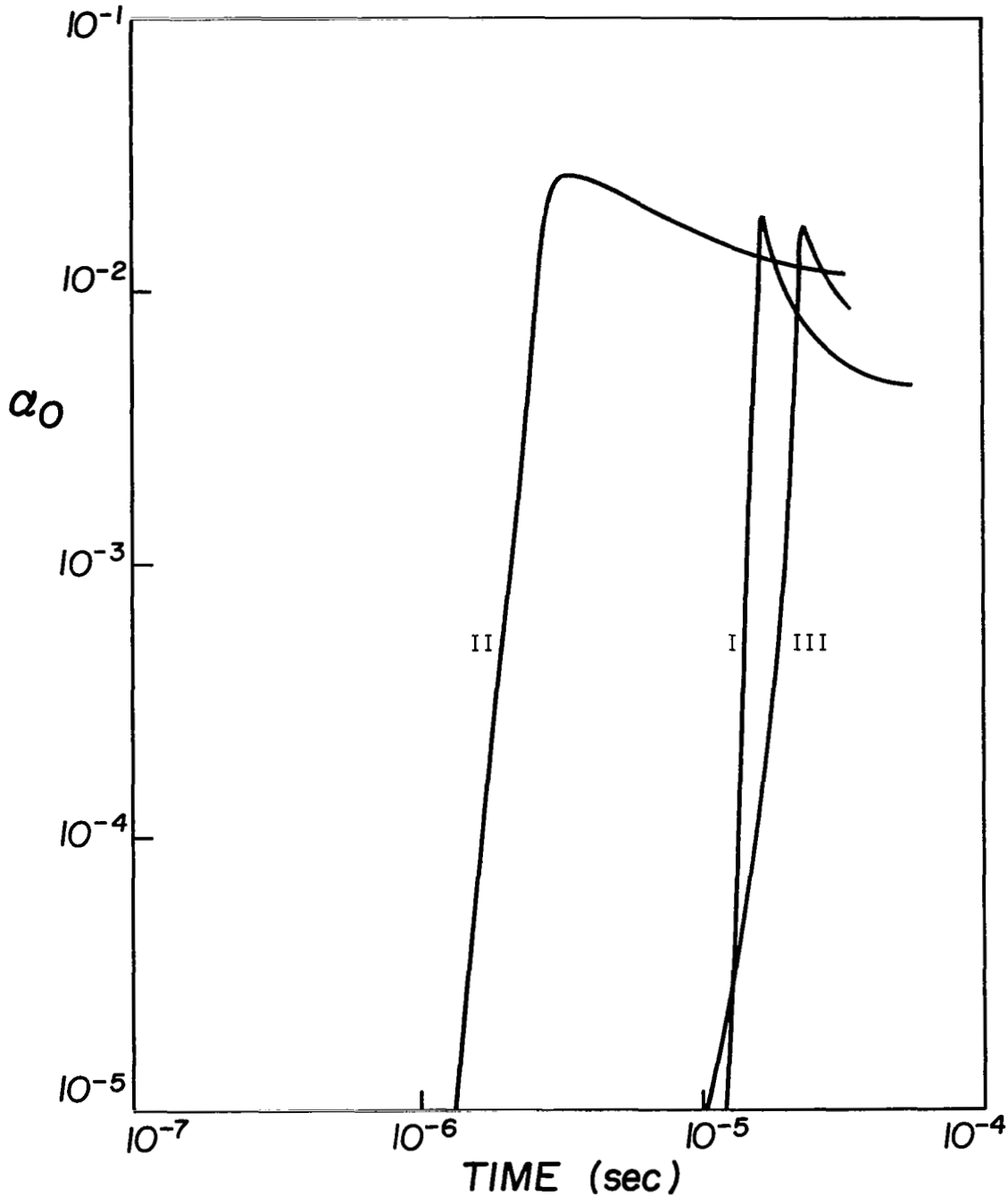

FIG. 2 VARIATION OF MASS FRACTION OF ATOMIC OXYGEN α_O IN STOICHIOMETRIC HYDROGEN-AIR MIXTURES AT CONSTANT PRESSURE.

CURVE I: P = 1.51 atm, T = 1340°K
CURVE II: P = 1 atm, T = 2000°K
CURVE III: P = 1 atm, T = 1140°K, Vitiated Air $\alpha_{H_2O\ init} = 0.15$

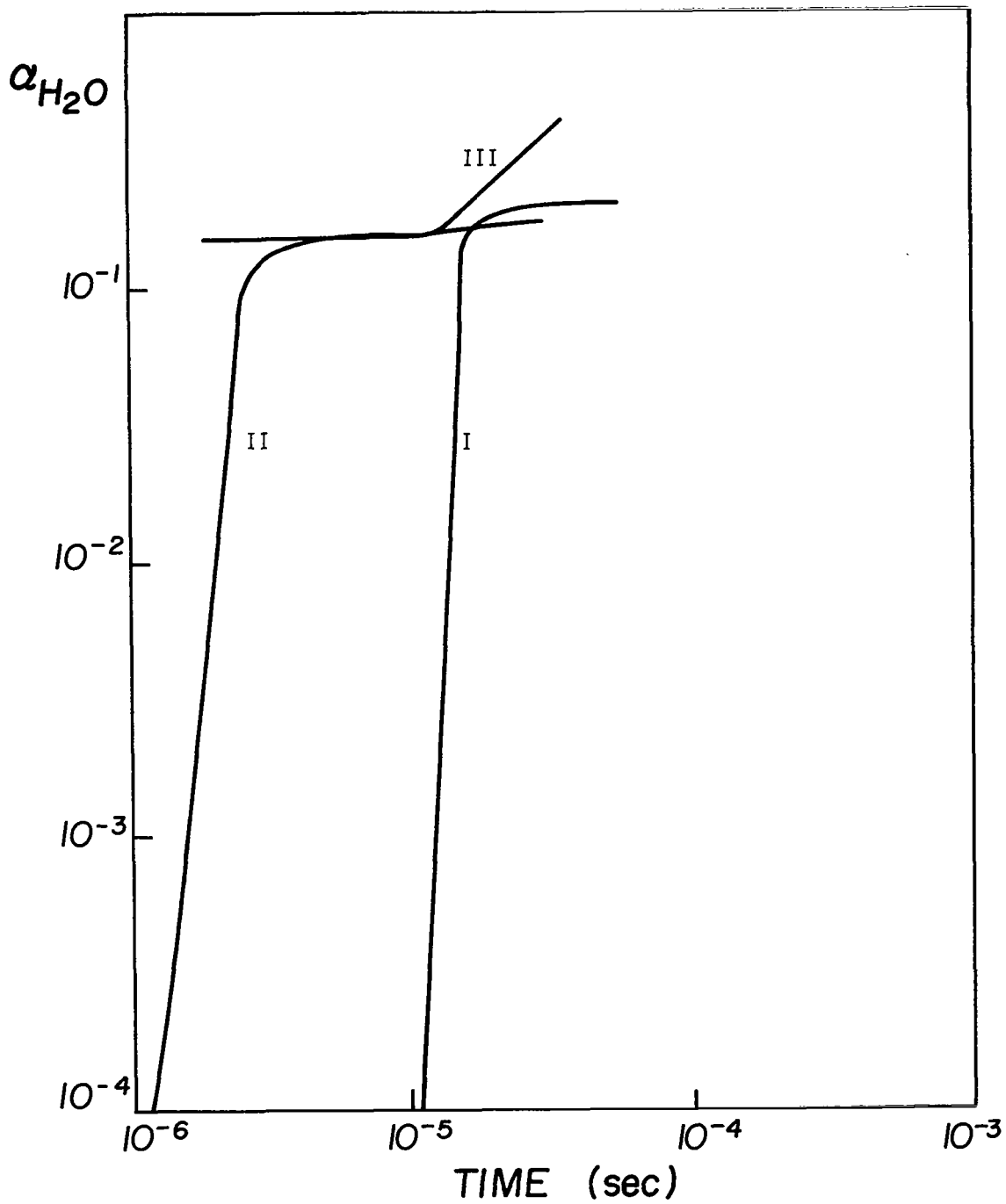

FIG. 3 VARIATION OF MASS FRACTION OF WATER α_{H_2O} IN STOICHIOMETRIC HYDROGEN-AIR MIXTURES AT CONSTANT PRESSURE.

CURVE I: P = 1.51 atm, T = 1340°K
CURVE II: P = 1 atm, T = 2000°K
CURVE III: P = 1 atm, T = 1140°K, Vitiated Air $\alpha_{H_2O\ init} = 0.15$

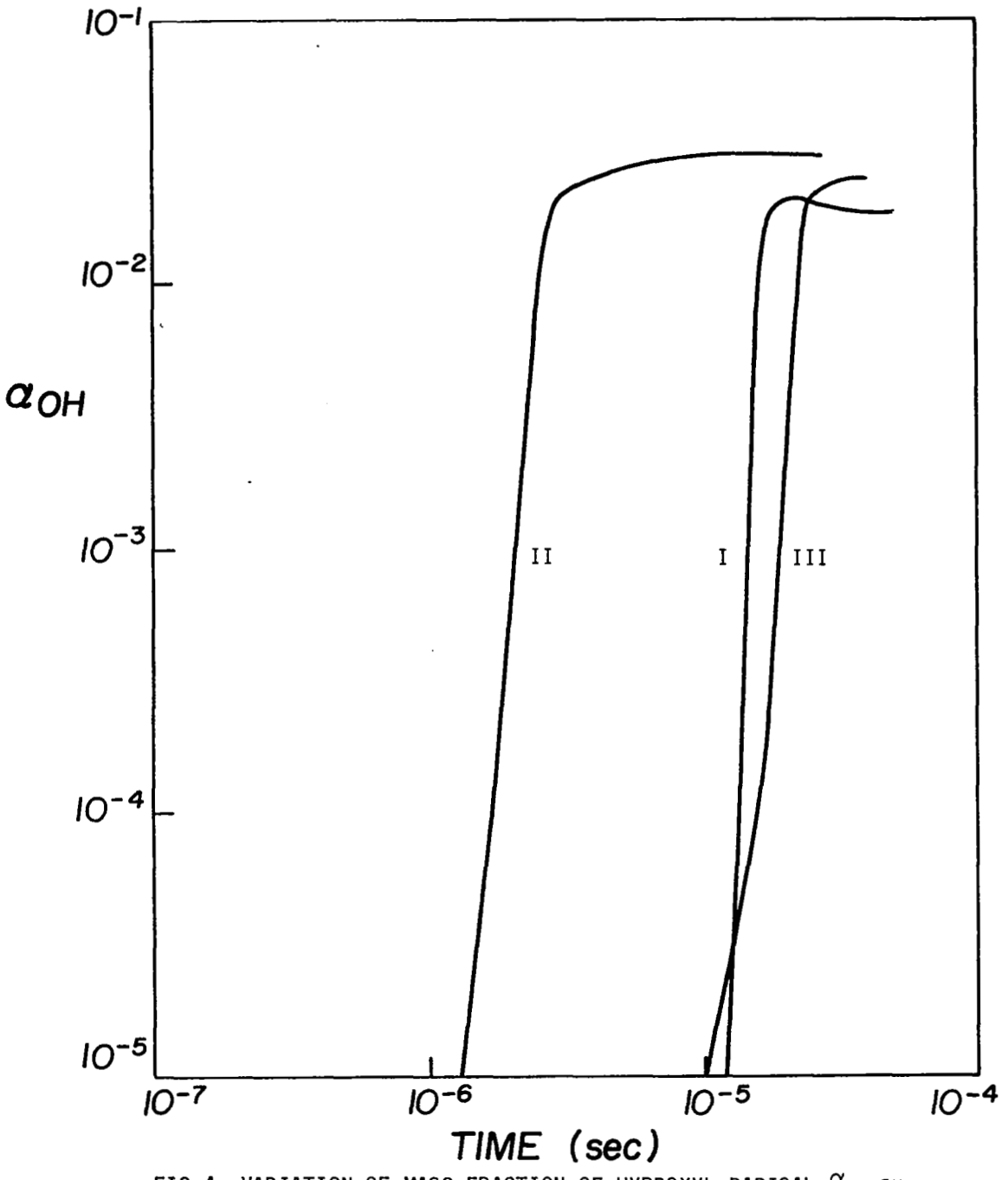

FIG. 4 VARIATION OF MASS FRACTION OF HYDROXYL RADICAL α_{OH} IN STOICHIOMETRIC HYDROGEN-AIR MIXTURES AT CONSTANT PRESSURE.

CURVE I: P = 1.51 atm, T = 1340°K
CURVE II: P = 1 atm, T = 2000°K
CURVE III: P = 1 atm, T = 1140°K, Vitiated Air $\alpha_{H_2O\ init} = 0.15$

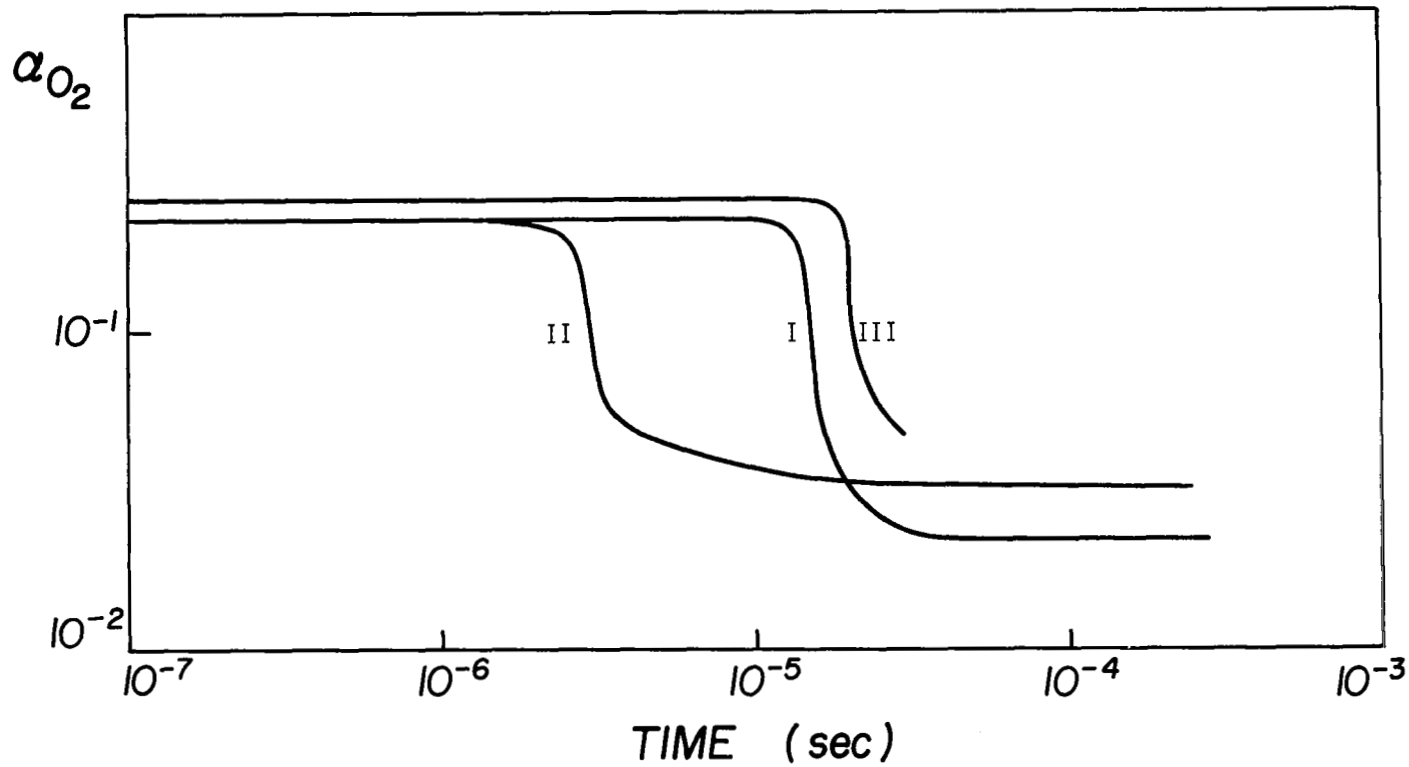

FIG. 5 VARIATION OF MASS FRACTION OF MOLECULAR OXYGEN α_{O_2} IN STOICHIOMETRIC HYDROGEN-AIR MIXTURES AT CONSTANT PRESSURE.

CURVE I: P = 1.51 atm, T = 1340°K
CURVE II: P = 1 atm, T = 2000°K
CURVE III: P = 1 atm, T = 1140°K, Vitiated Air $\alpha_{H_2O\ init} = 0.15$

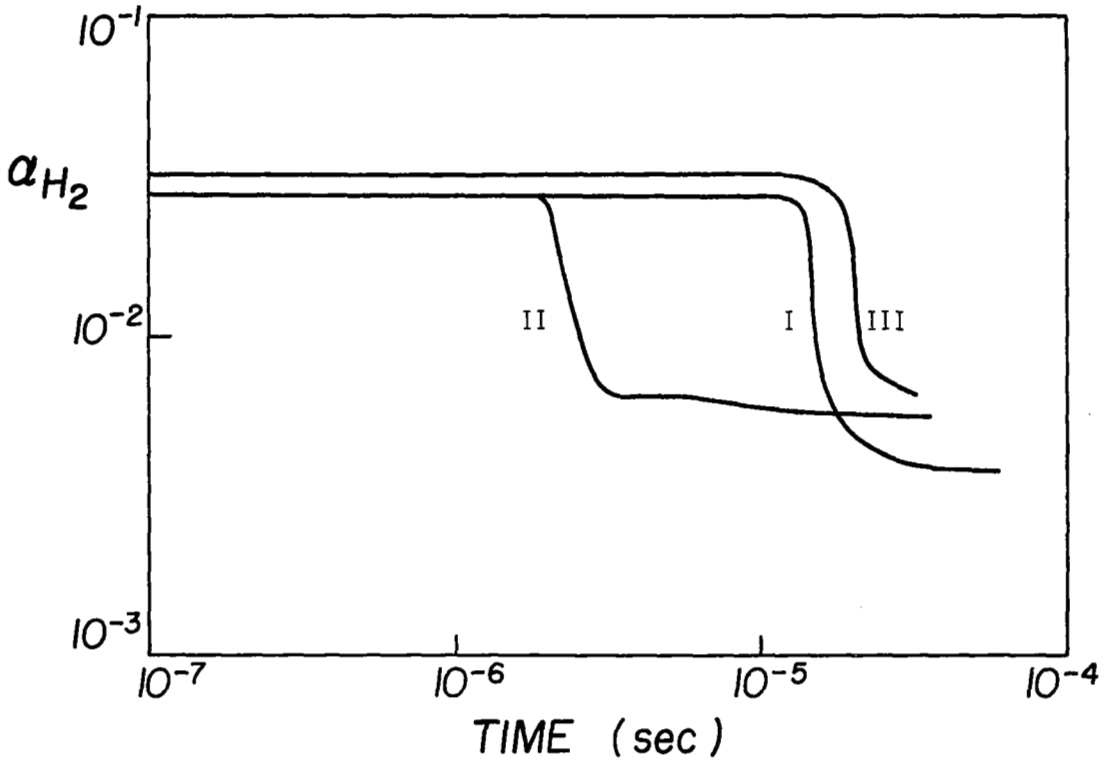

FIG. 6 VARIATION OF MASS FRACTION OF MOLECULAR HYDROGEN α_{H_2} IN STOICHIOMETRIC HYDROGEN-AIR MIXTURES AT CONSTANT PRESSURE.

CURVE I: P = 1.51 atm, T = 1340°K
CURVE II: P = 1 atm, T = 2000°K
CURVE III: P = 1 atm, T = 1140°K, Vitiated Air $\alpha_{H_2O\ init} = 0.15$

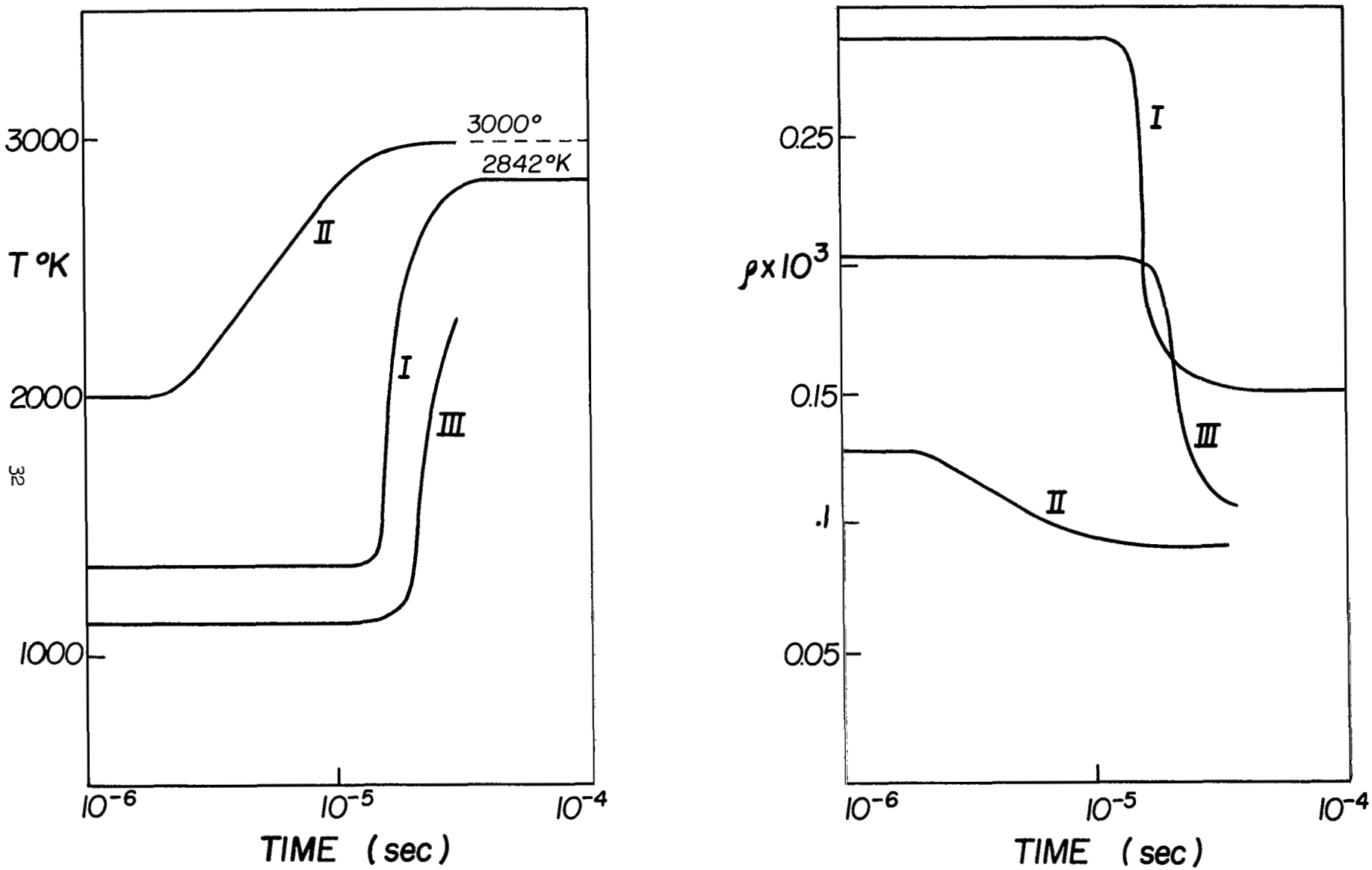

FIG. 7 VARIATION OF TEMPERATURE AND DENSITY IN STOICHIOMETRIC HYDROGEN-AIR MIXTURES AT CONSTANT PRESSURE.

CURVE I: P = 1.51 atm, T = 1340°K
CURVE II: P = 1 atm, T = 2000°K
CURVE III: P = 1 atm, T = 1140°K, Vitiated Air $\alpha_{H_2O\ init} = 0.15$

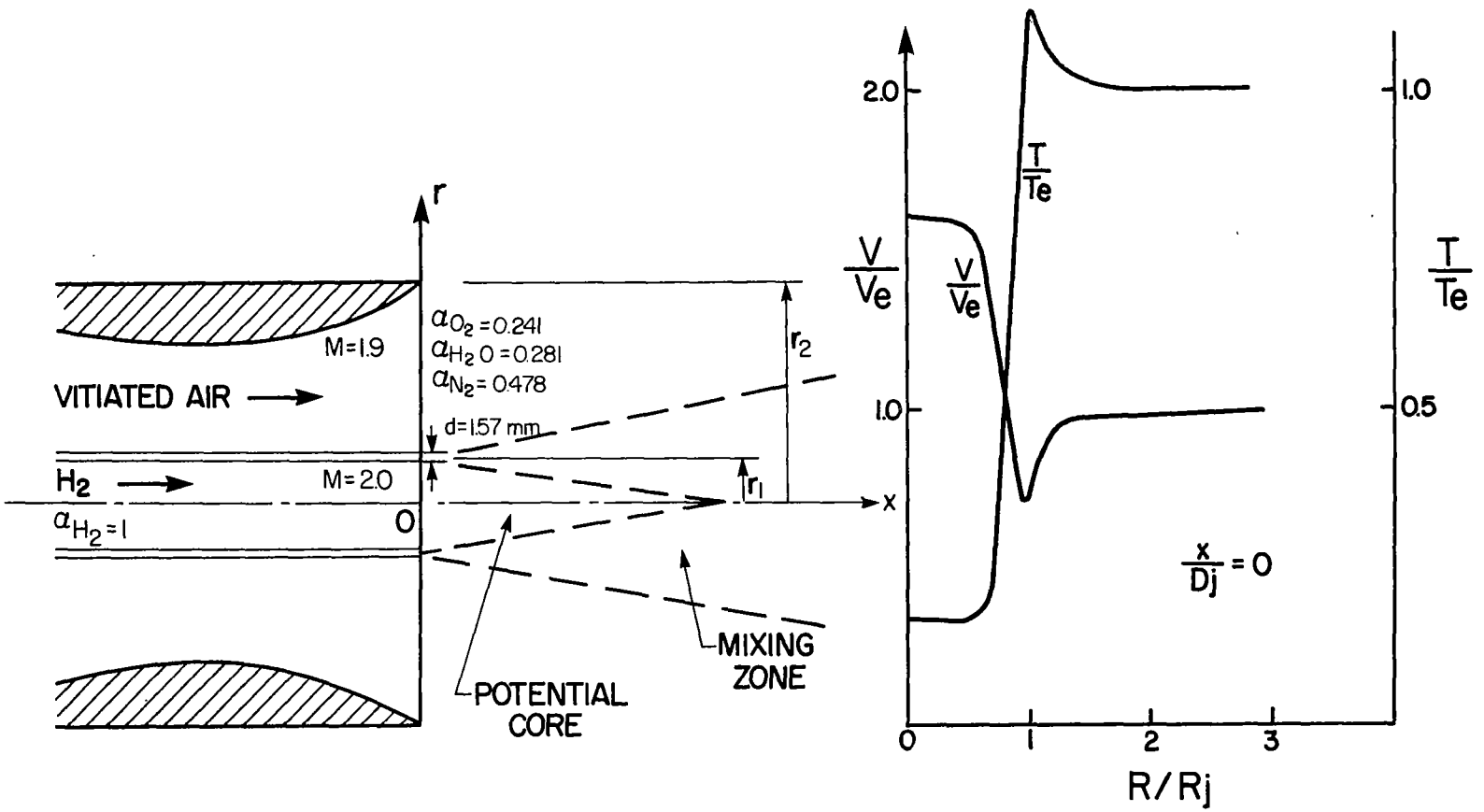

r_1 = 0.00476 m r_2 = 0.0325 m P = 1 atm V_e = 1510 m/s , T_e = 1533°K

FIG. 8 SCHEMATIC DIAGRAM OF THE AXISYMMETRIC TURBULENT FREE MIXING FLOW FIELD WITH COMBUSTION AND INITIAL PROFILES

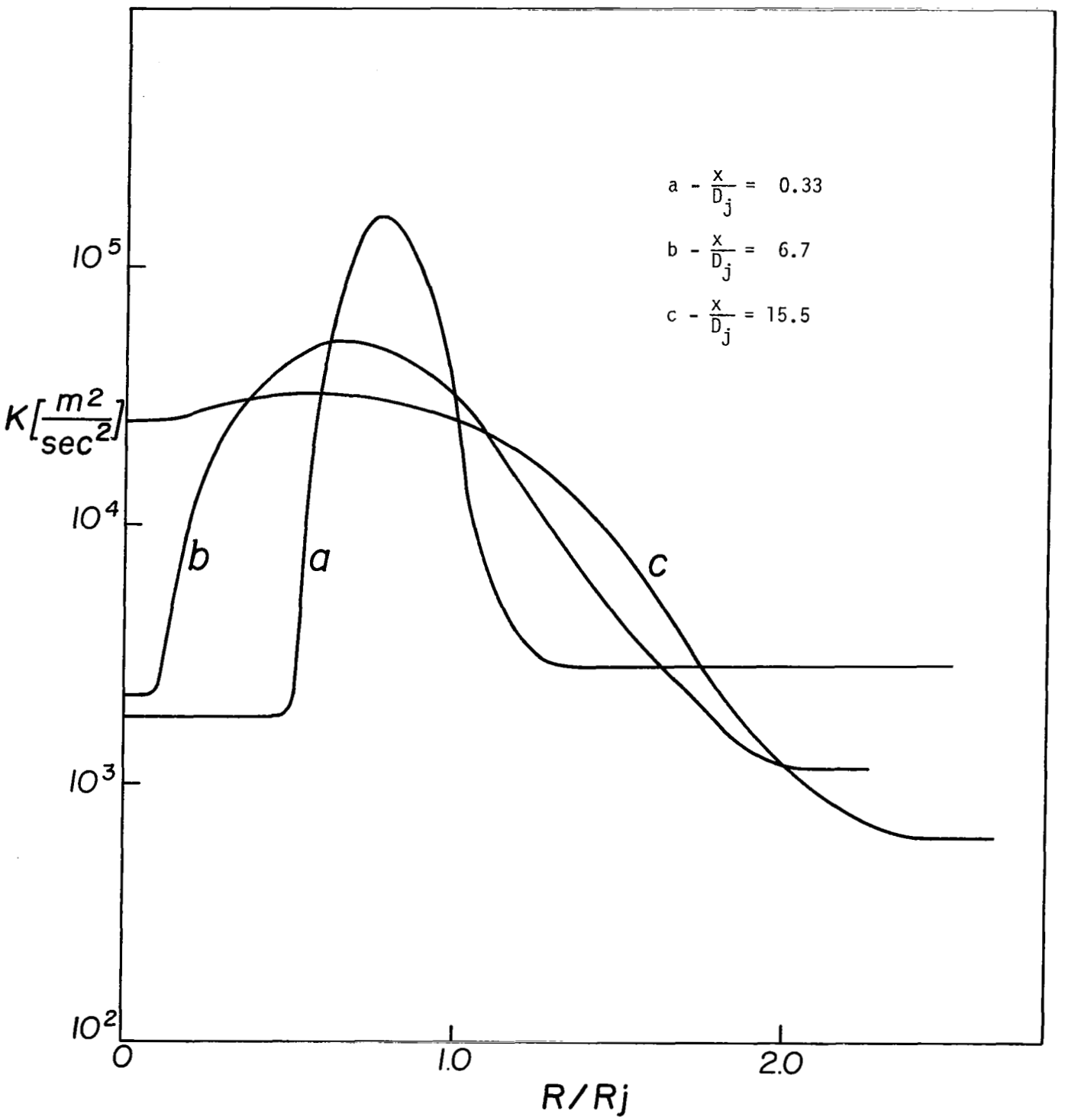

FIG. 9 RADIAL TURBULENT KINETIC ENERGY PROFILE

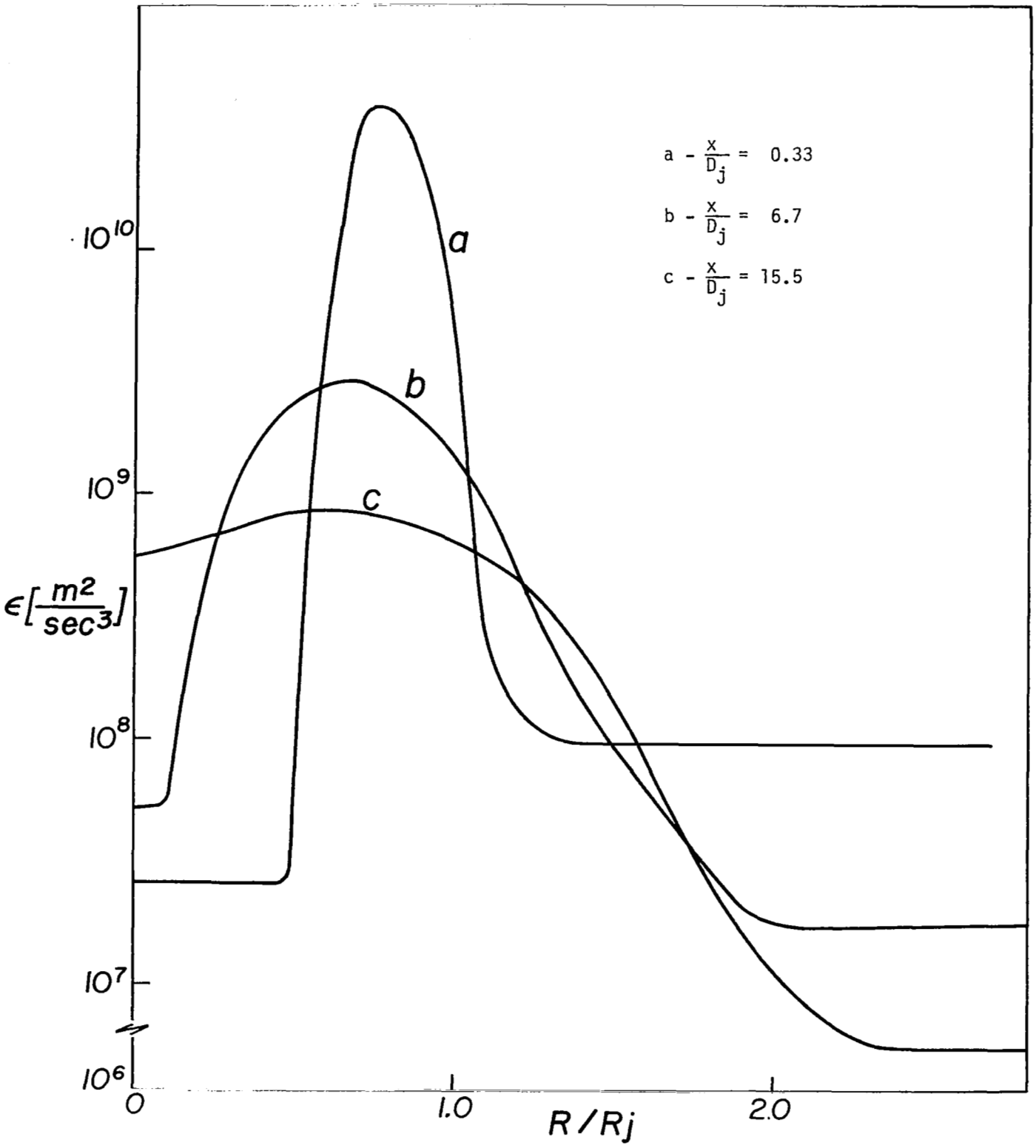

FIG. 10 RADIAL TURBULENT-DISSIPATION PROFILE

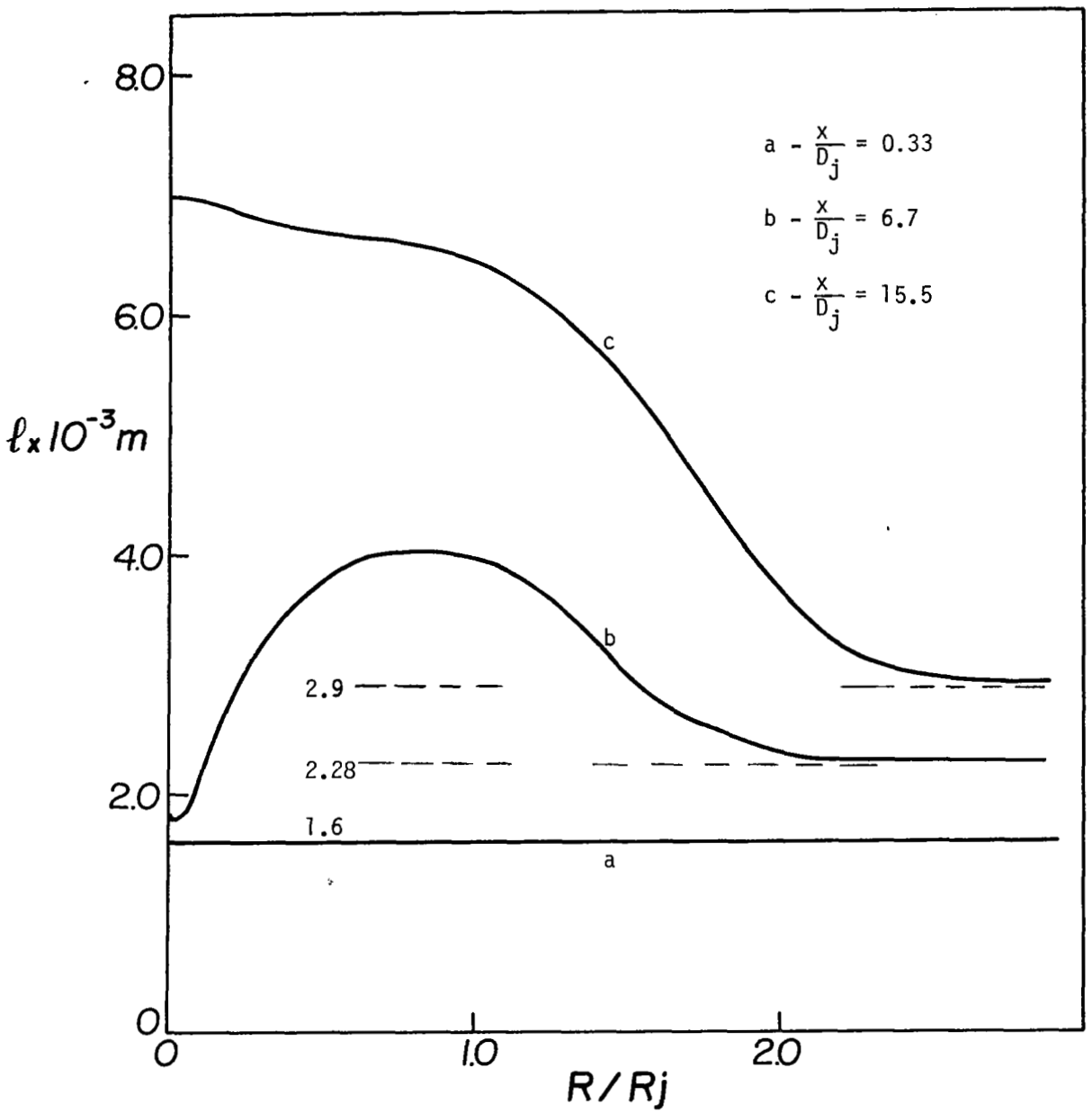

FIG. 11 RADIAL TURBULENCE LENGTH SCALE PROFILE

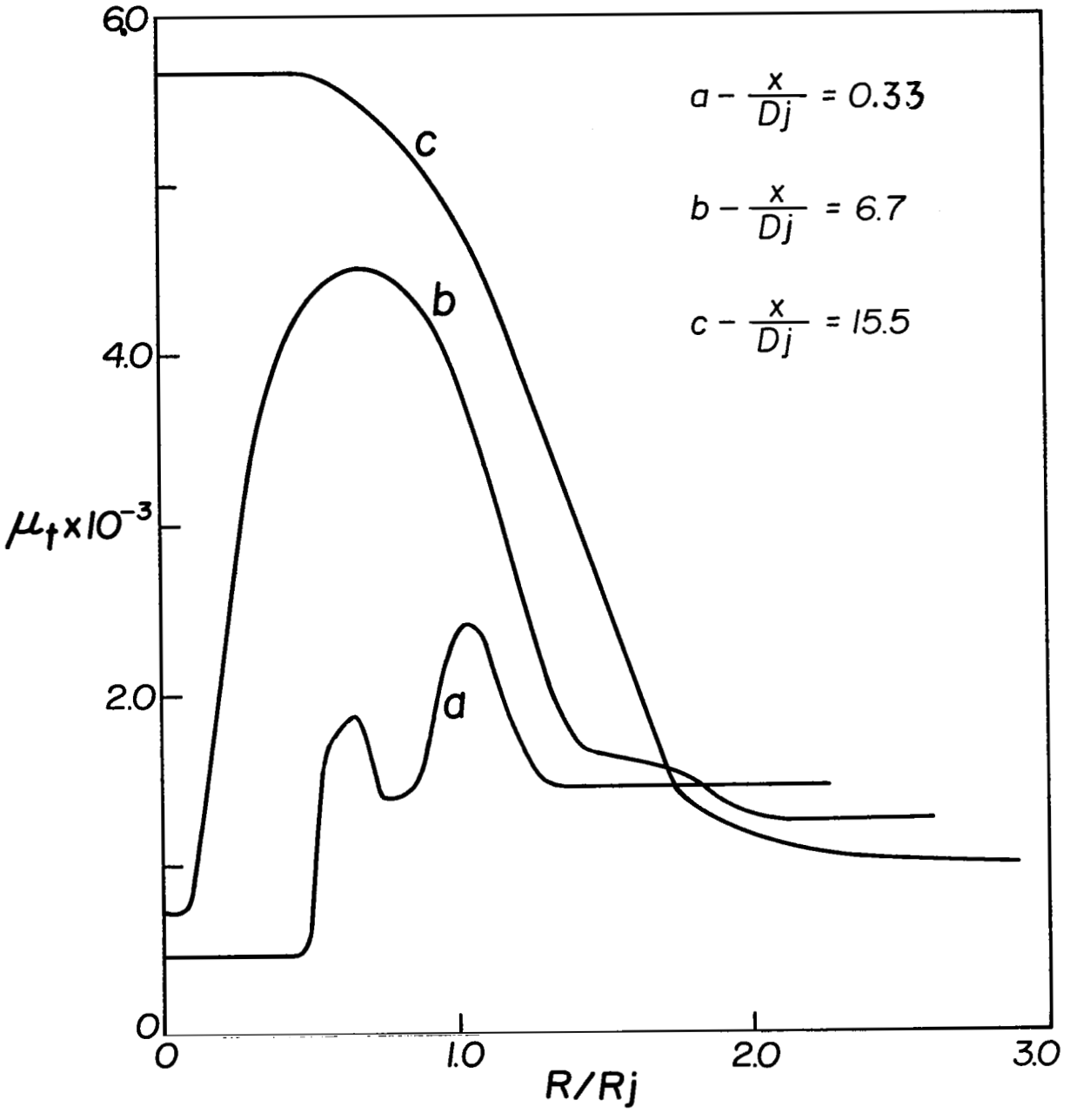

FIG. 12 RADIAL TURBULENT VISCOSITY PROFILE

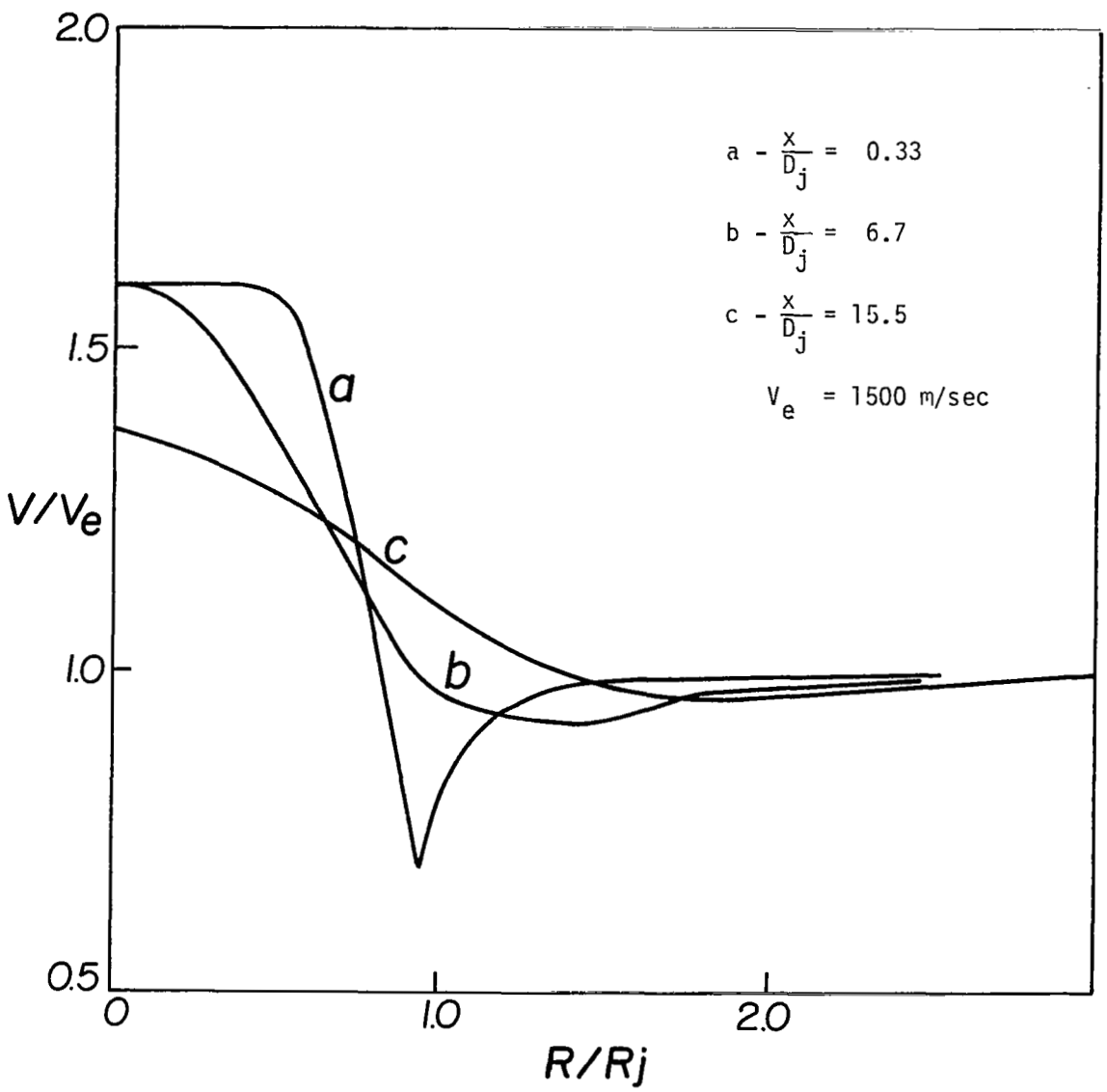

FIG. 13 RADIAL VELOCITY PROFILES

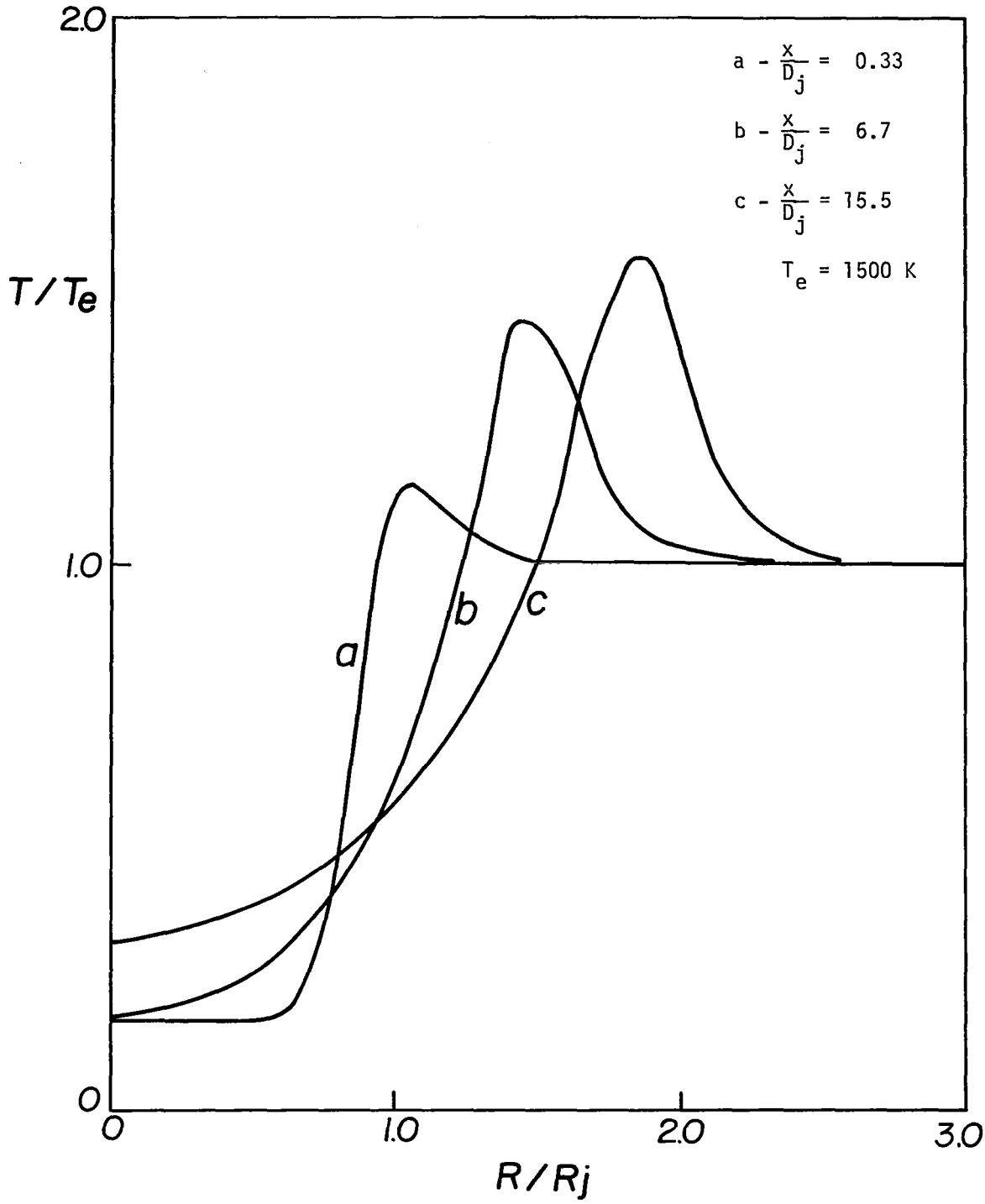

FIG. 14 RADIAL TEMPERATURE PROFILES

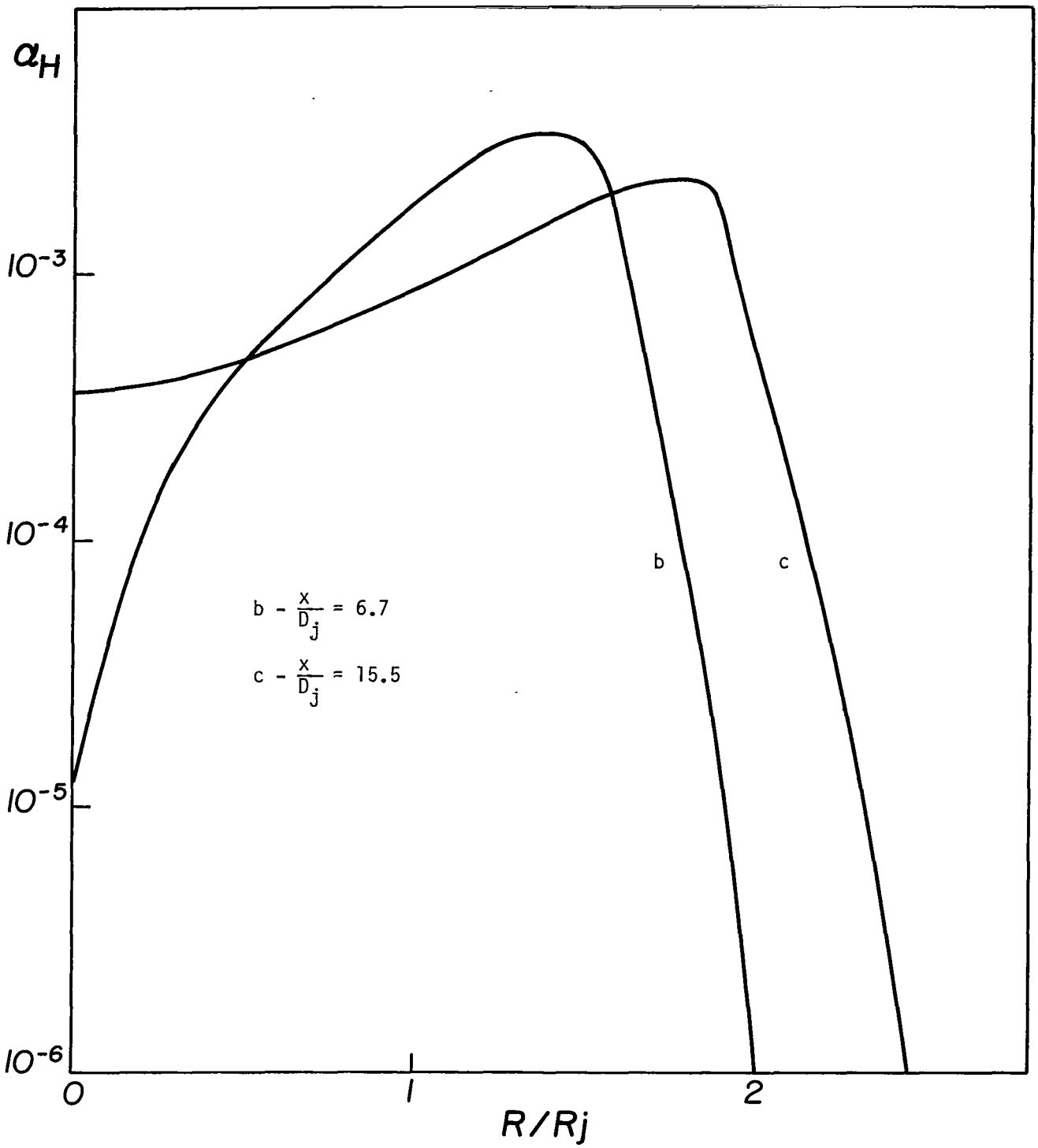

FIG. 15 RADIAL MASS FRACTION PROFILES OF ATOMIC HYDROGEN

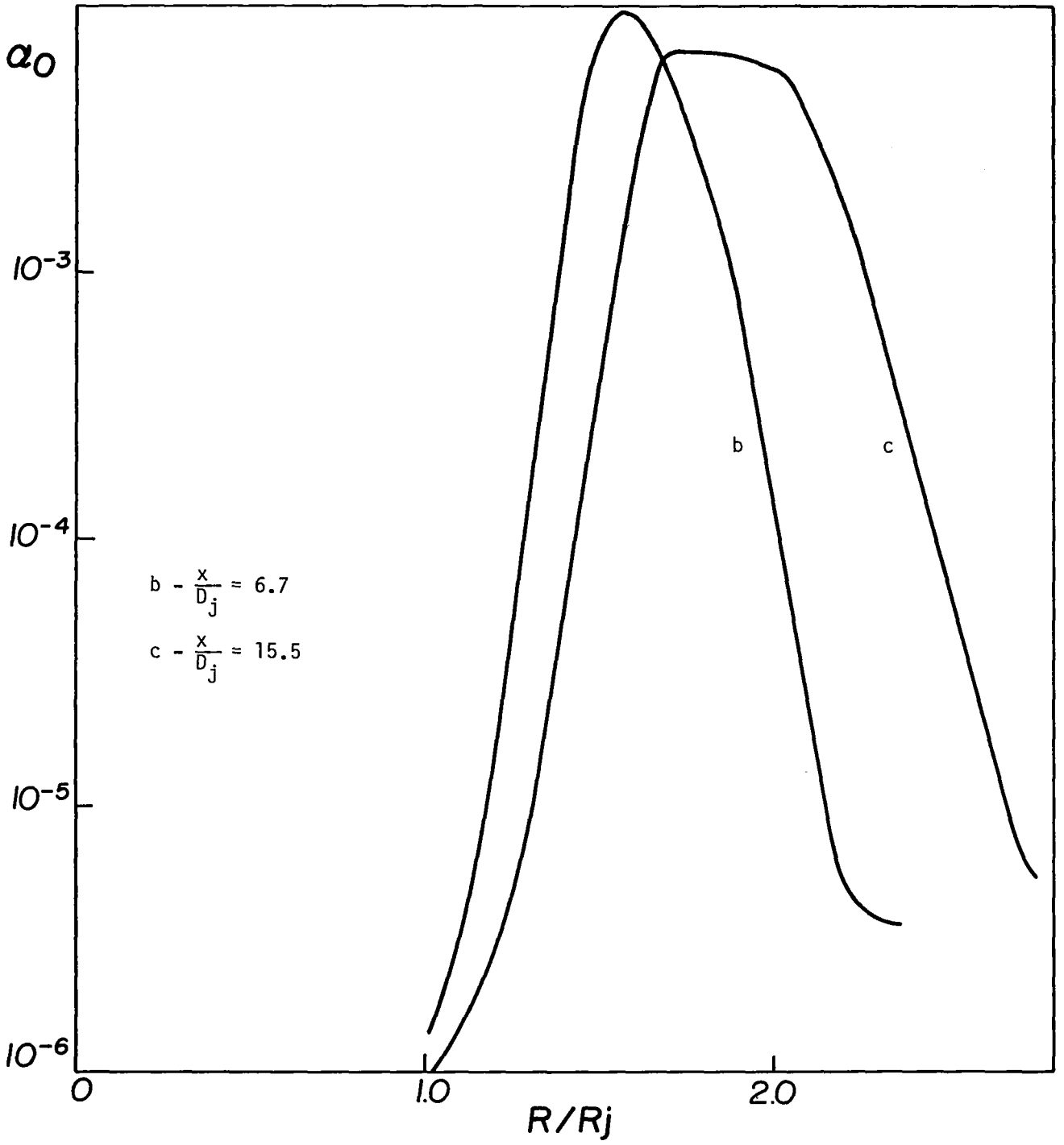

FIG. 16 RADIAL MASS FRACTION PROFILES OF ATOMIC OXYGEN

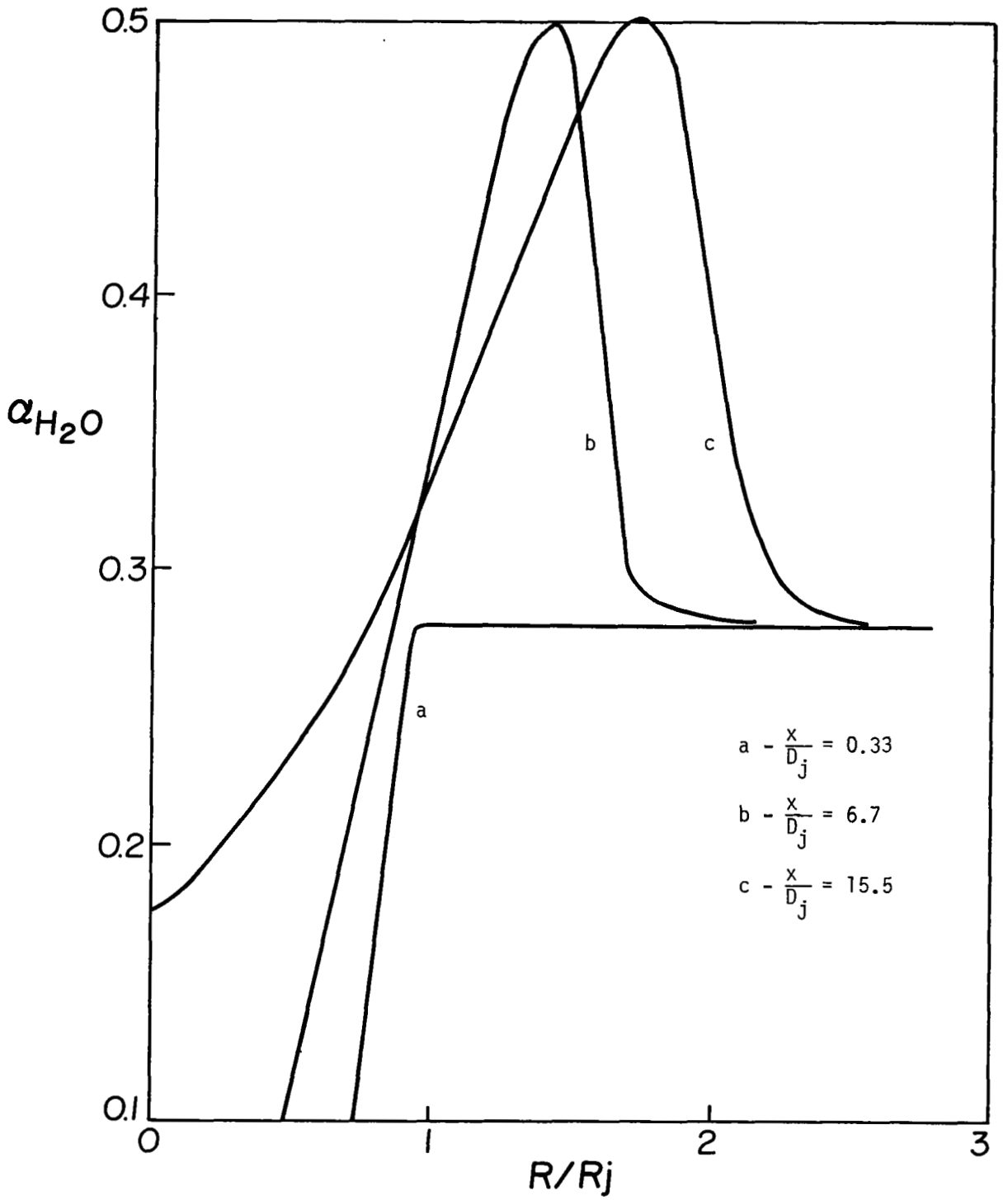

FIG. 17 RADIAL MASS FRACTION PROFILES OF WATER

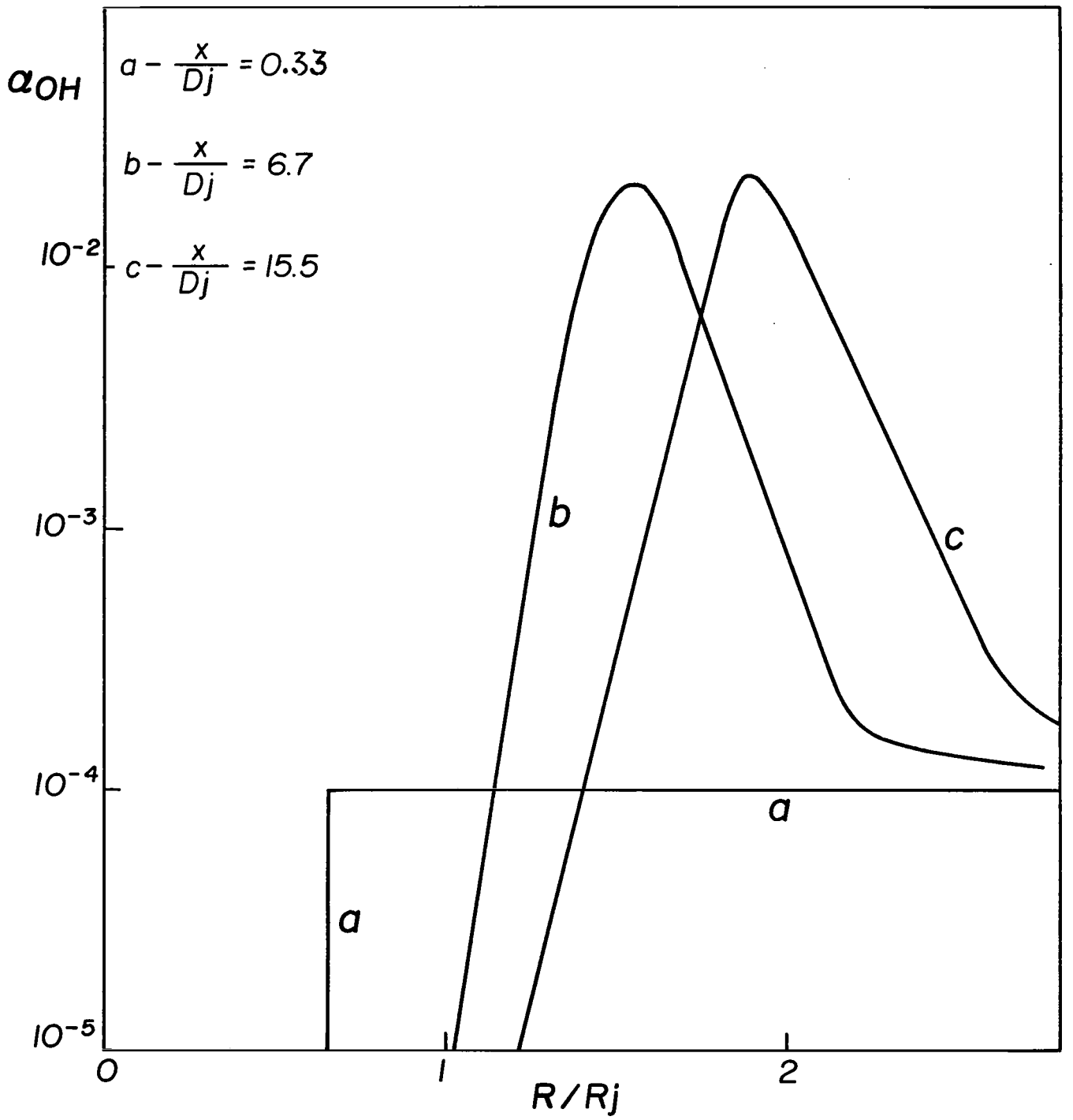

FIG. 18 RADIAL MASS FRACTION PROFILES OF OH.

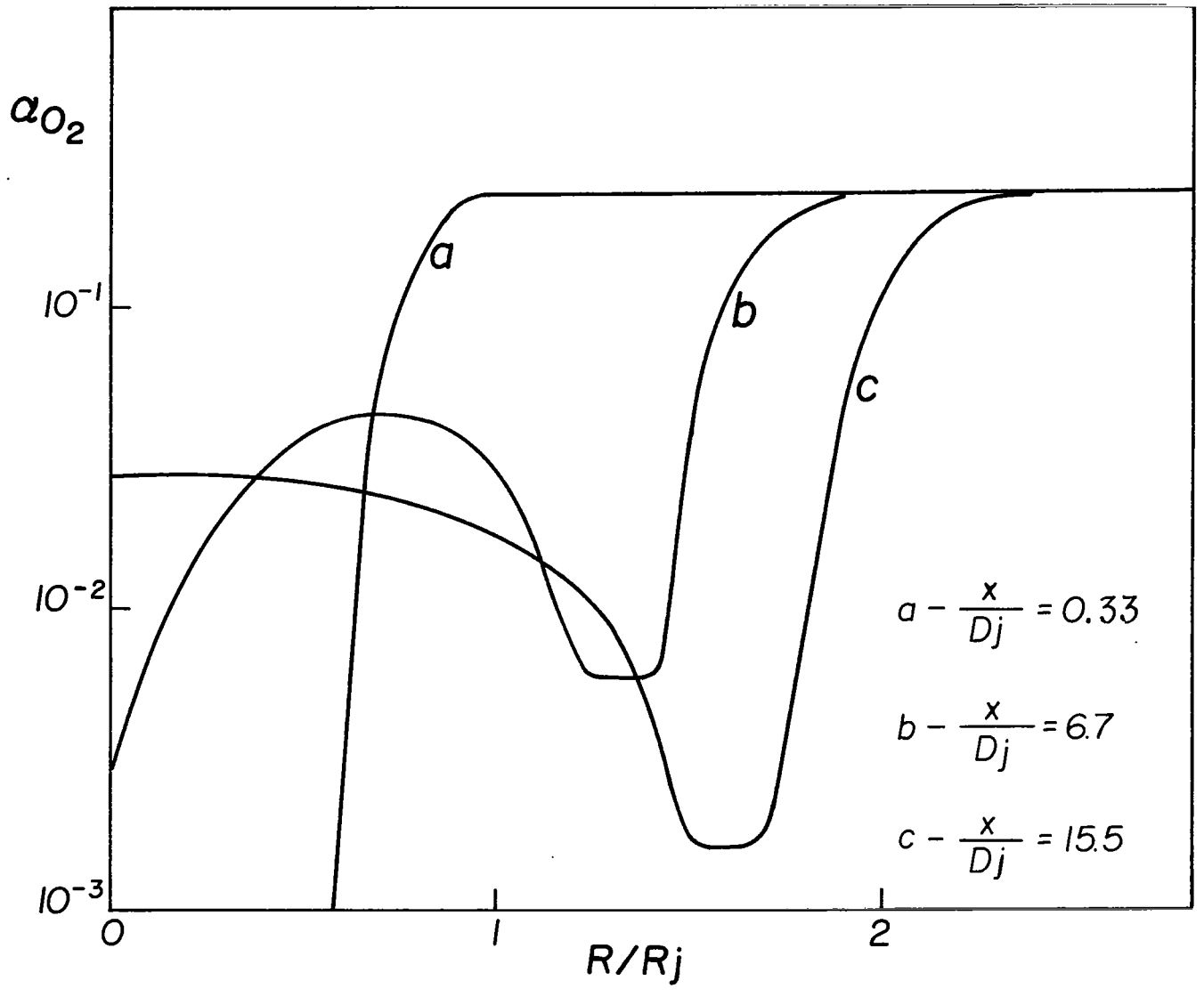

FIG. 19 RADIAL MASS FRACTION PROFILES OF MOLECULAR OXYGEN

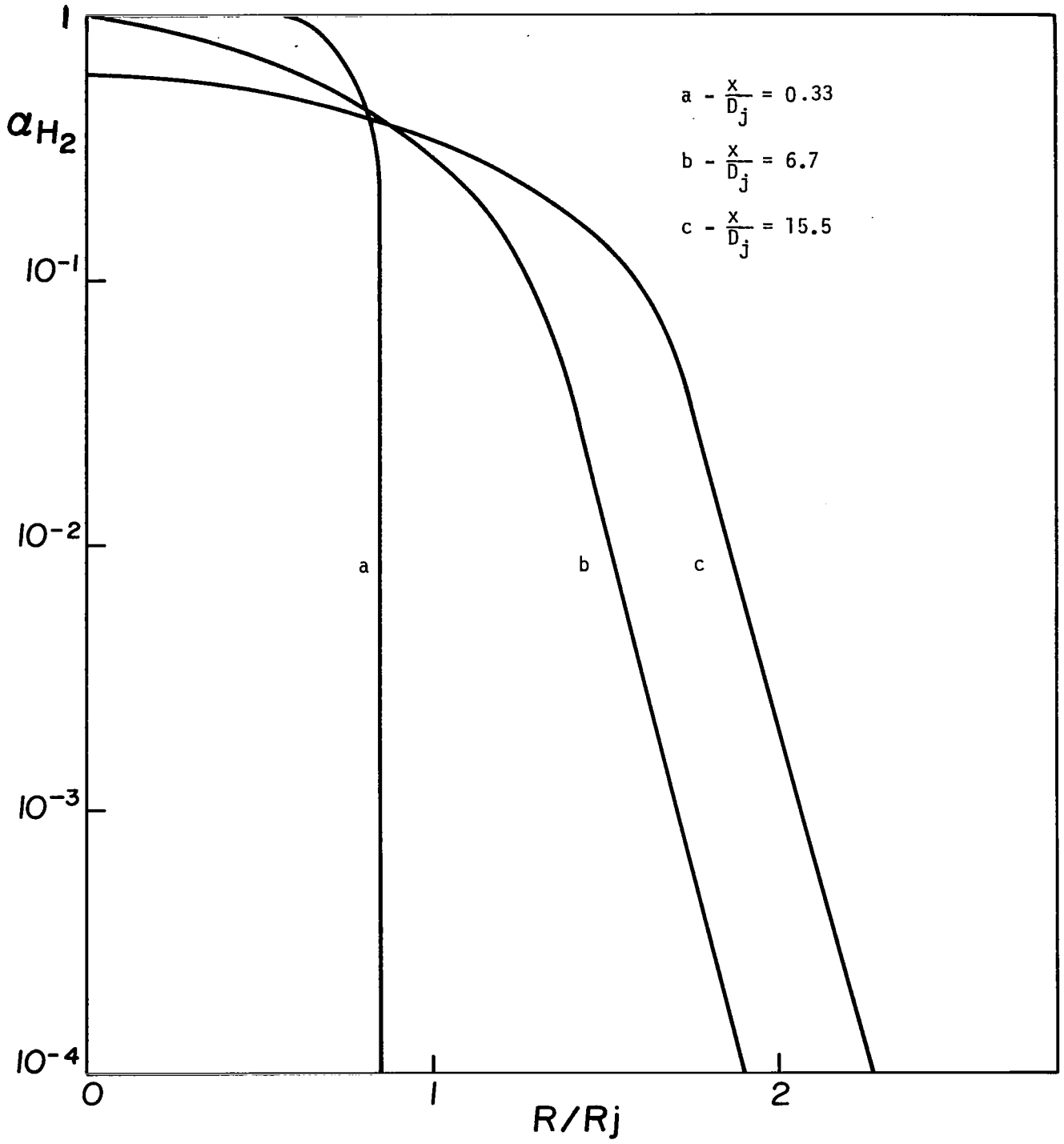

FIG. 20 RADIAL MASS FRACTION PROFILES OF MOLECULAR HYDROGEN

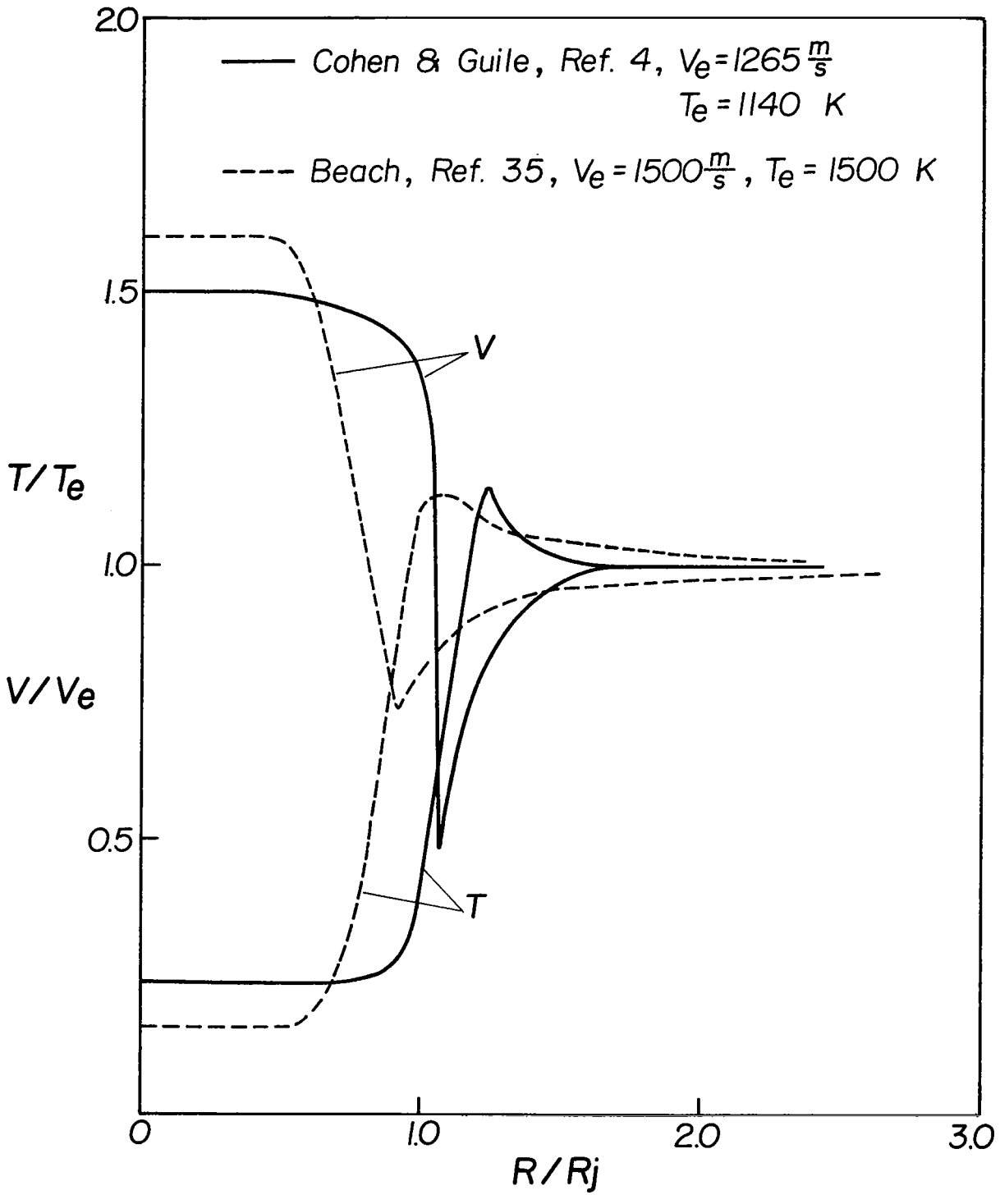

FIG. 21 INITIAL RADIAL VELOCITY AND TEMPERATURE PROFILES

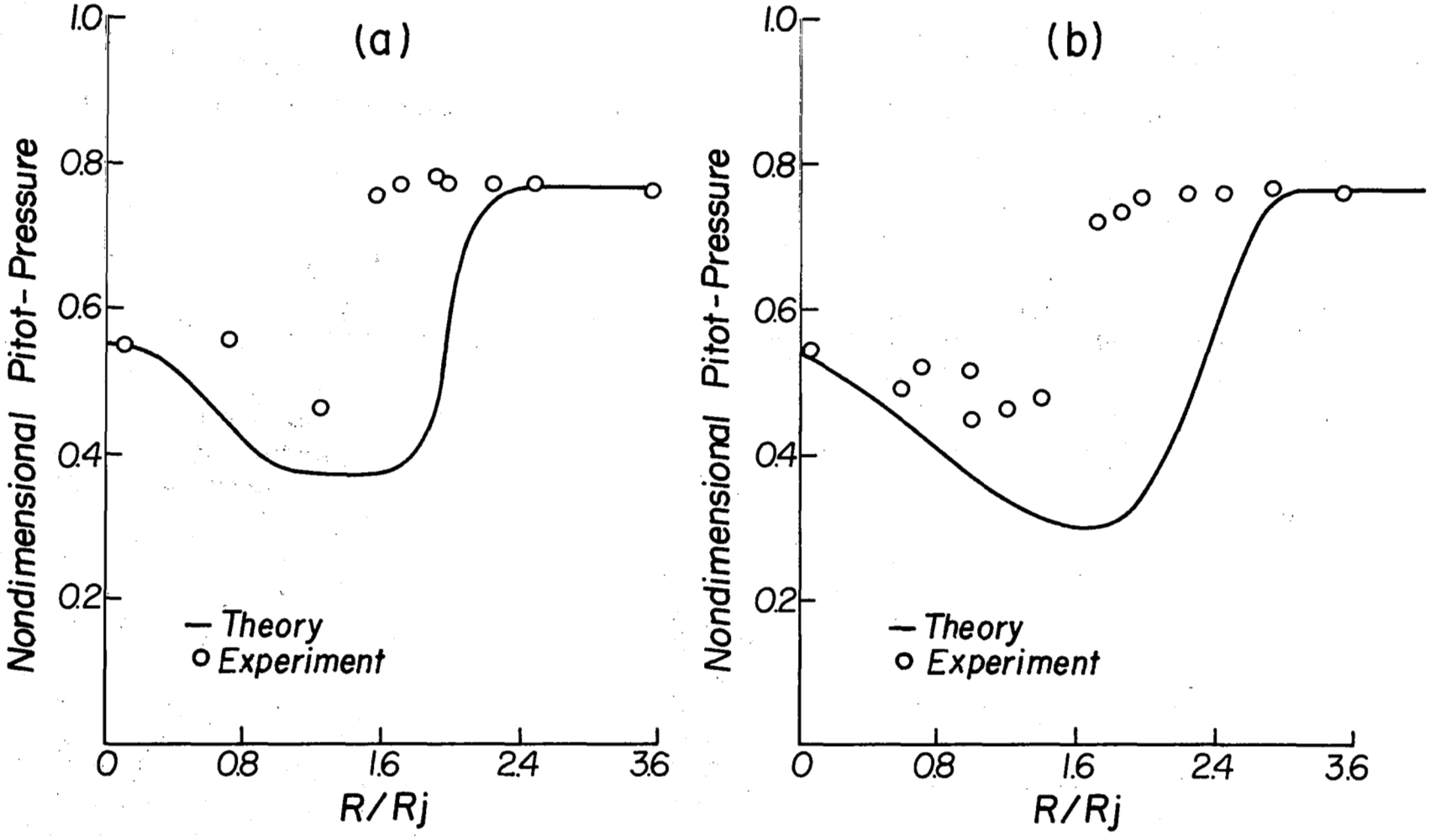

FIG. 22 RADIAL NONDIMENSIONAL PITOT-PRESSURE PROFILE, P_{ref} = 5.55 atm

(a) Cohen & Guile, x/D_j = 5.2, (b) Cohen & Guile, x/D_j = 8.9

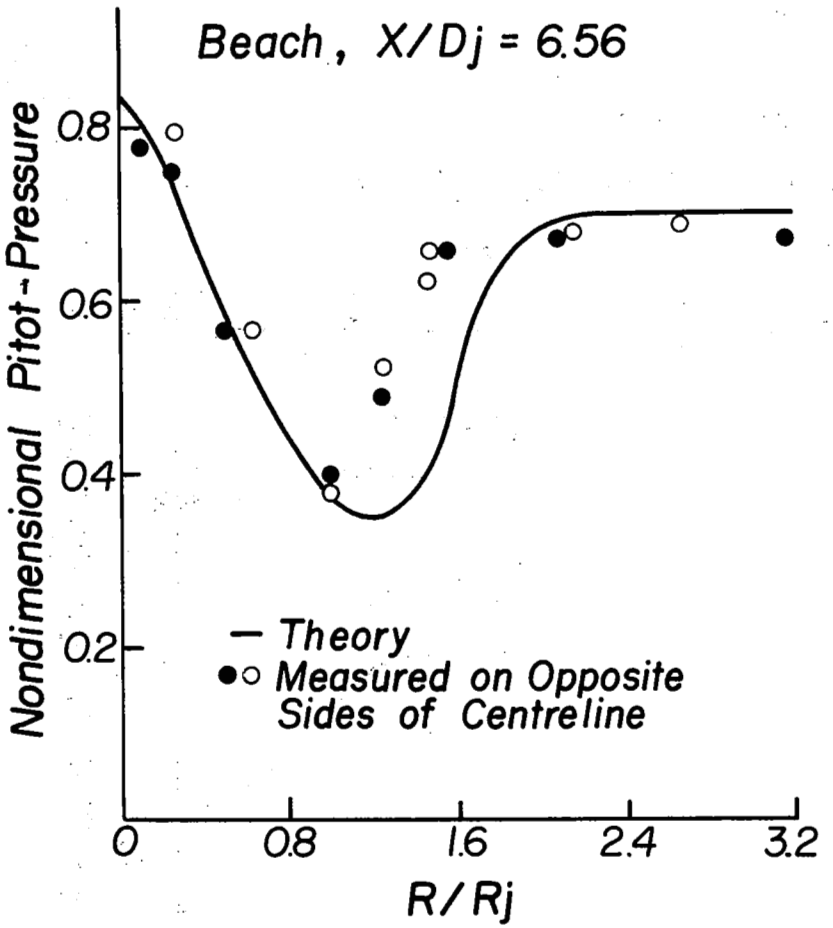

FIG. 23 RADIAL NONDIMENSIONAL PITOT-PRESSURE PROFILE
P_{ref} = 6.66 atm

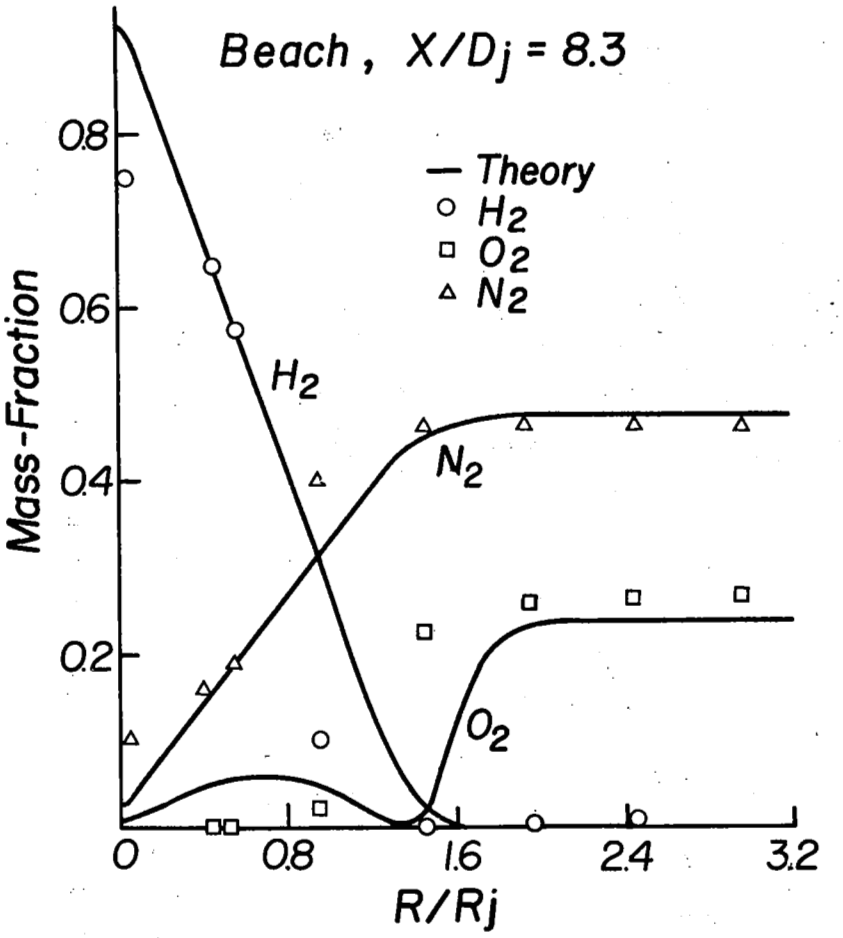

FIG. 24 RADIAL MASS FRACTION PROFILE OF N_2, O_2 AND H_2

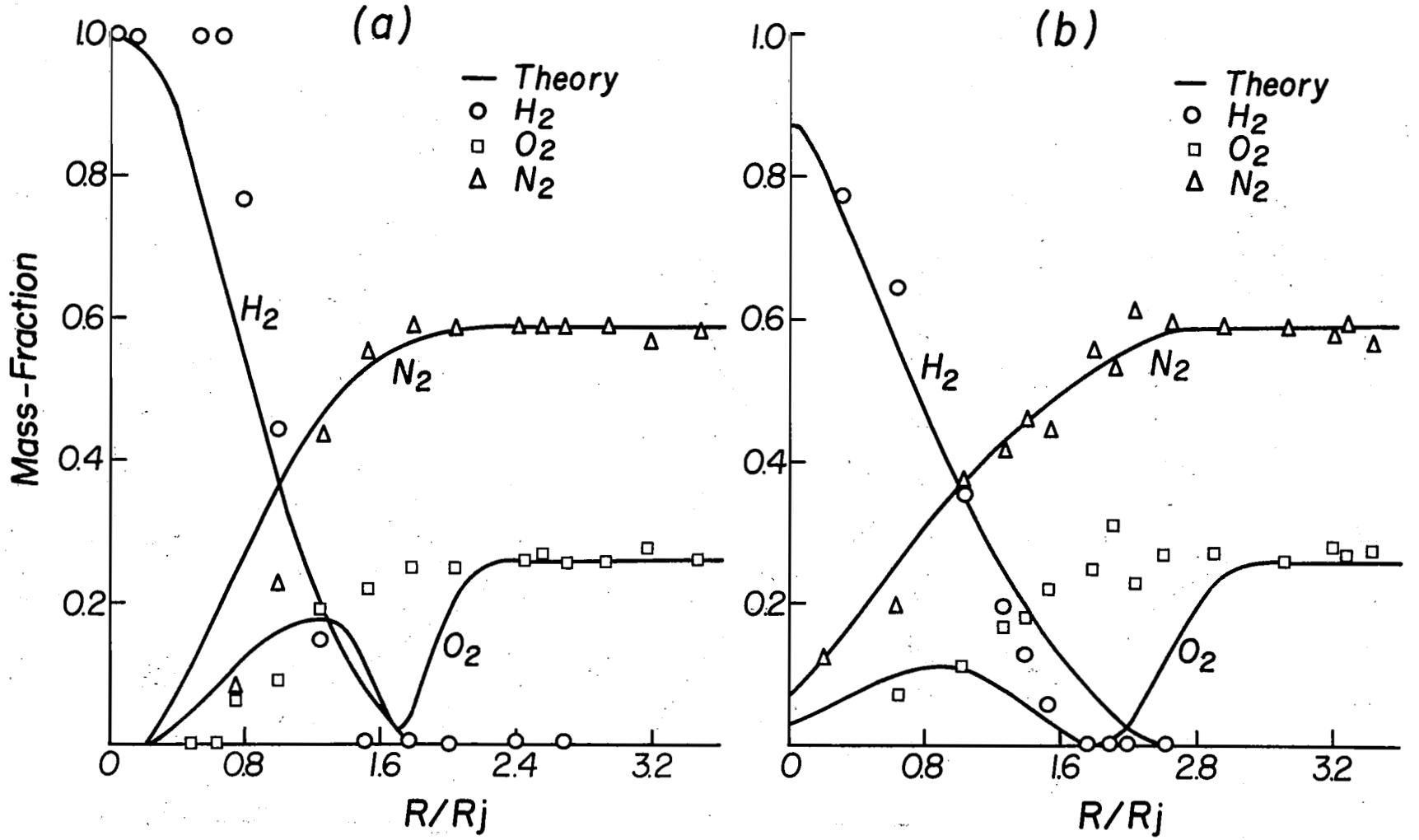

FIG. 25 RADIAL MASS-FRACTION PROFILE OF N_2, O_2 AND H_2

(a) Cohen & Guile, $x/D_j = 5.2$, (b) Cohen & Guile, $x/D_j = 8.9$

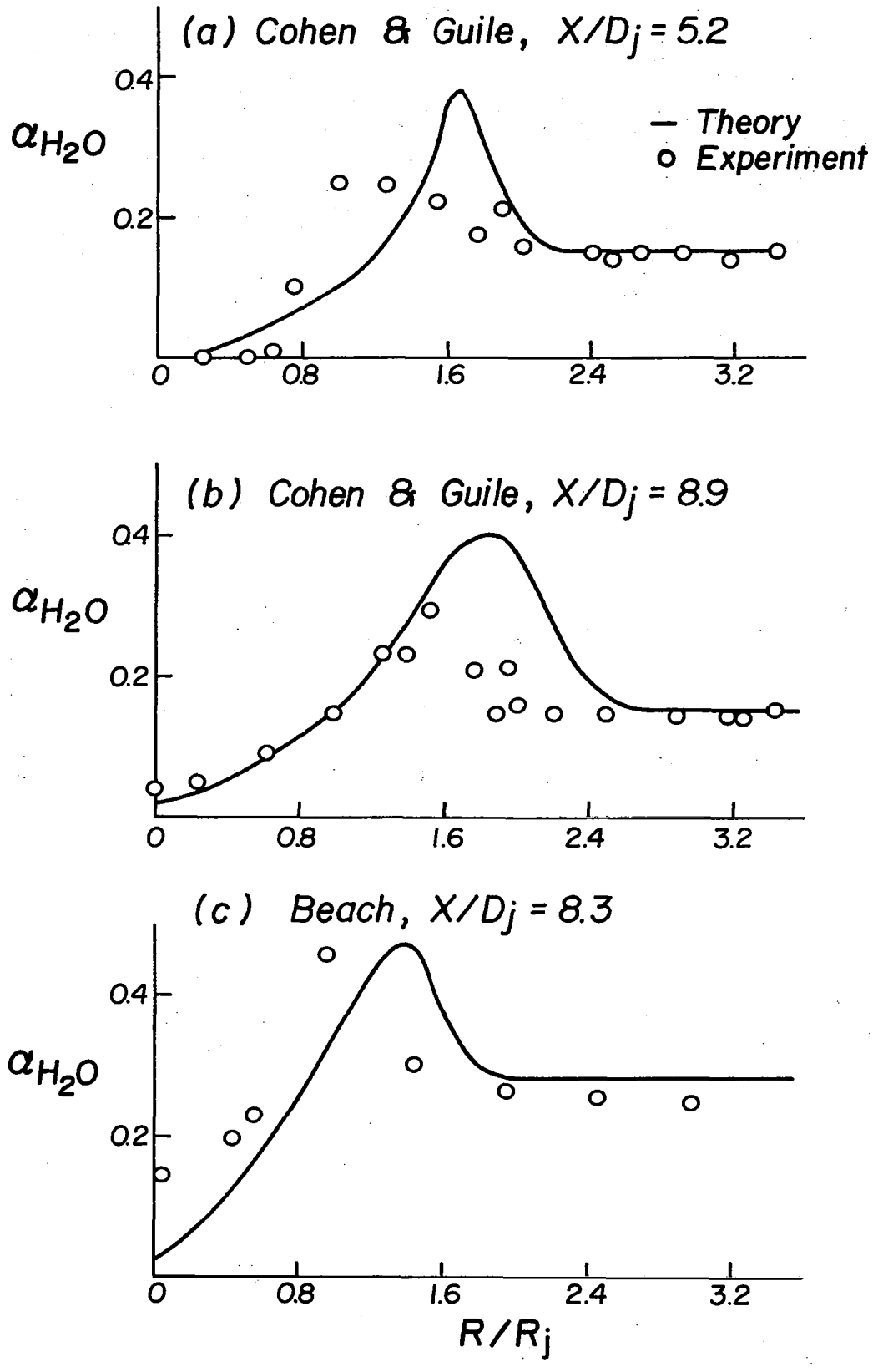

FIG. 26 RADIAL MASS-FRACTION PROFILES OF WATER

1. Report No.	2. Government Accession No.	3. Recipient's Catalog No.
NASA CR-3024		

4. Title and Subtitle	5. Report Date
ANALYSIS OF TURBULENT FREE JET HYDROGEN-AIR DIFFUSION FLAMES WITH FINITE CHEMICAL REACTION RATES	August 1978
	6. Performing Organization Code
7. Author(s)	8. Performing Organization Report No.
J. P. Sislian	UTIAS Report 224
	10. Work Unit No.
9. Performing Organization Name and Address	11. Contract or Grant No.
University of Toronto Institute for Aerospace Studies 4925 Dufferin Street Downsview, Ontario, Canada, M3H 5T6	NAS1-14843
	13. Type of Report and Period Covered
12. Sponsoring Agency Name and Address	Contractor Report
National Aeronautics & Space Administration Washington, DC 20546	14. Sponsoring Agency Code

15. Supplementary Notes

Langley Technical Monitor: John S. Evans, Jr.
Final Report

16. Abstract

The nonequilibrium flow field resulting from the turbulent mixing and combustion of a supersonic axisymmetric hydrogen jet in a supersonic parallel coflowing air stream is analyzed. Effective turbulent transport properties are determined using the (k-ε) model. The finite-rate chemistry model considers eight reactions between six chemical species, H, O, H_2O, OH, O_2, and H_2. The governing set of nonlinear partial differential equations is solved by an implicit finite-difference procedure.

Radial distributions are obtained at two downstream locations of variables such as turbulent kinetic energy, turbulent dissipation rate, turbulent scale length, and viscosity. The results show that these variables attain peak values at the axis of symmetry. Computed distributions of velocity, temperature, and mass fraction are also given.

A direct analytical approach to account for the effect of species-concentration fluctuations on the mean production rate of species (the phenomenon of unmixedness) is also presented. However, the use of the method does not seem justified in view of the excessive computer time required to solve the resulting system of equations.

17. Key Words (Suggested by Author(s))	18. Distribution Statement
Finite rate chemistry Unmixedness	Unclassified - Unlimited Subject Category 34

19. Security Classif. (of this report)	20. Security Classif. (of this page)	21. No. of Pages	22. Price*
Unclassified	Unclassified	58	$5.25

* For sale by the National Technical Information Service, Springfield, Virginia 22161

NASA-Langley, 1978